ARMY RESEARCH LABORATORY

Dynamic Response of Composite Gun Tubes Subjected to a Moving Internal Pressure

Jerome T. Tzeng
David A. Hopkins

ARL-TR-889   October 1995

DTIC
SELECTED
OCT 3 0 1995
G

19951026 070

DTIC QUALITY INSPECTED 5

NOTICES

Destroy this report when it is no longer needed. DO NOT return it to the originator.

Additional copies of this report may be obtained from the National Technical Information Service, U.S. Department of Commerce, 5285 Port Royal Road, Springfield, VA 22161.

The findings of this report are not to be construed as an official Department of the Army position, unless so designated by other authorized documents.

The use of trade names or manufacturers' names in this report does not constitute indorsement of any commercial product.

REPORT DOCUMENTATION PAGE

Public reporting burden for this collection of information is estimated to average 1 hour per response, including the time for reviewing instructions, searching existing data sources, gathering and maintaining the data needed, and completing and reviewing the collection of information. Send comments regarding this burden estimate or any other aspect of this collection of information, including suggestions for reducing this burden, to Washington Headquarters Services, Directorate for Information Operations and Reports, 1215 Jefferson Davis Highway, Suite 1204, Arlington, VA 22202-4302, and to the Office of Management and Budget, Paperwork Reduction Project(0704-0188), Washington, DC 20503.

1. AGENCY USE ONLY (Leave blank)	2. REPORT DATE October 1995	3. REPORT TYPE AND DATES COVERED Final, Jun 94 - Jul 95

4. TITLE AND SUBTITLE
Dynamic Response of Composite Gun Tubes Subjected to a Moving Internal Pressure

5. FUNDING NUMBERS
NAVY R1191/5WPRS

6. AUTHOR(S)
Jerome T. Tzeng and David A. Hopkins

7. PERFORMING ORGANIZATION NAME(S) AND ADDRESS(ES)
U.S. Army Research Laboratory
ATTN: AMSRL-WT-PD
Aberdeen Proving Ground, MD 21005-5066

8. PERFORMING ORGANIZATION REPORT NUMBER
ARL-TR-889

9. SPONSORING/MONITORING AGENCY NAMES(S) AND ADDRESS(ES)
U.S. Naval Surface Warfare Center
Dahlgren, VA 22448-9999

10. SPONSORING/MONITORING AGENCY REPORT NUMBER

11. SUPPLEMENTARY NOTES
This work was supported by the U.S. Naval Surface Warfare Center, Dahlgren, Virginia, through the FIREFOX program.

12a. DISTRIBUTION/AVAILABILITY STATEMENT
Approved for public release; distribution is unlimited.

12b. DISTRIBUTION CODE

13. ABSTRACT (Maximum 200 words)

The dynamic response of a composite gun tube subjected to a moving pressure front is investigated. The flexural wave in the wall of the gun tube is modeled using both closed-form analytic and finite element methods. Results indicate that very high-amplitude and high-frequency strains are induced in the gun tube at the instant and location of projectile passage as the velocity of moving pressure front approaches the fundamental propagation velocity of the flexural wave. The dynamic effects are especially critical on overwrapped composite gun barrels because of the multi-material construction, anisotropy of material properties, potential thermal degradation of the composite materials due to gas propellant, and the design goals inherent in lightweight structure applications. Finally, this study illustrates the importance of dynamics fracture mechanisms in lightweight ballistic engineering applications. These results also illustrate some of the potential shortcomings of the static analysis methodology traditionally used in gun barrel design.

14. SUBJECT TERMS
dynamic strain, composite cylinders

15. NUMBER OF PAGES
39

16. PRICE CODE

17. SECURITY CLASSIFICATION OF REPORT	18. SECURITY CLASSIFICATION OF THIS PAGE	19. SECURITY CLASSIFICATION OF ABSTRACT	20. LIMITATION OF ABSTRACT
UNCLASSIFIED	UNCLASSIFIED	UNCLASSIFIED	UL

NSN 7540-01-280-5500

Standard Form 298 (Rev. 2-89)
Prescribed by ANSI Std. 239-18   298-102

INTENTIONALLY LEFT BLANK.

ACKNOWLEDGMENT

Accesion For		
NTIS CRA&I		☒
DTIC TAB		☐
Unannounced		☐
Justification		
By		
Distribution /		
Availability Codes		
Dist	Avail and / or Special	
A-1		

INTENTIONALLY LEFT BLANK.

TABLE OF CONTENTS

INTENTIONALLY LEFT BLANK.

LIST OF FIGURES

INTENTIONALLY LEFT BLANK.

1. INTRODUCTION

Very high-amplitude and high-frequency strains develop in a gun tube at the instant and location of projectile passage. The ballistic community refers to this phenomena as dynamic strain amplification. It is caused by resonance of flexural waves with the moving pressure front as the pressure front approaches a critical propagation velocity of the flexural waves in the gun tube. The dynamic response of a tube subjected to moving pressure loads has been investigated by Taylor (1942), Jones and Bhuta (1964), Tang (1965), and Reismann (1965). More recently, Simkins (1987) investigated the response of flexural waves in constant cross-section tank gun tubes, while evidence of dynamic strain amplification in the 120-mm tank guns was observed. Hopkins (1991) used the finite element method to study the dynamic strain response in realistic and complex cylindrical geometries subjected to a moving pressure front for which analytic solutions are not available. Currently, research in the dynamic strain effect in cylinders has been limited to tubes made of isotropic materials and unit-material constructions. This report investigates the dynamic response in an overwrapped composite tube with a steel liner. The results apply to lightweight composite gun tube design.

The radial expansion (deformation) of the tube subjected to internal pressure can travel as wave propagation along the tube dynamically. The velocity of propagation depends on the matieral properties and geometry of the gun tube. When the velocity of a projectile approaches the propagation velocity of radial expansion, the deformation is amplified due to resonance. The stress and strain levels due to dynamic strain amplification can be two to three times higher than those attained under static loading conditions. As the projectile travels down the tube, there is local shell bending caused by the pressure discontinuity at the pressure front. The deformation due to shell bending leads to very high axial and transverse shear stresses. The transverse shear stress magnitude is critical, since the shear strength of composites is generally much lower than the shear strength of metals. The dynamic cyclic strains, due to the resonance, may cause fatigue of the composite materials and eventually lead to fracture of the overwrapped tube.

This dynamic strain effect is especially critical for overwrapped composite gun tubes that are designed to achieve enhanced performance with relatively light weight. From a design point of view, the weight savings, in general, decrease the rigidity and inertia of the tubes under dynamic loads. These effects are especially critical at the muzzle, where the tube's wall thickness is the thinnest. The response at the interface between the composite overwrap and steel liner is important since the shear properties and tensile peel strength at this interface are low, due to relatively weak adhesion between composite and steel. The

1

thermal degradation of composite materials is also critical since the tube will be subjected to an elevated temperature during gun firing.

2. ANALYSIS

In this section, the dynamic response of a composite overwrapped gun tube subjected to a moving pressure load is investigated using both closed-form analytic and finite element methods. The critical velocity at which resonance occurs depends on the specific tube geometry and material properties. Except for simple geometries, it is not possible to obtain a closed-form expression for the critical velocity as a function of these parameters. As a first approximation though, Love's thin-shell theory can be used to derive a closed-form expression for the critical velocity. This is because predicted values of the critical velocity based on the thin-shell theory are reasonably accurate when compared with both experimentally measured values as well as values obtained using finite element methods. A rule-of-mixture approach for determining appropriate material properties is applied to simplify the calculation procedure for a multi-material construction. The finite element solution is obtained using a version of the DYNA2D (Hallquist 1987) hydrocode, which has been modified to allow accurate modeling of the moving pressure front. This approach allows modeling both the moving pressure front and the composite gun tube geometry in sufficient detail to simulate the actual loading conditions during the launch cycle.

2.1 <u>Critical Velocity</u>. As stated previously, the critical velocity of a flexural wave in a cylindrical tube can be obtained from Love's thin-shell theory. Although some assumptions of the thin-shell theory are not strictly valid for the gun tube's actual variable cross-section geometry, the prediction does provide a good estimation of the critical velocity. Additionally, the closed-form solution is very valuable in illustrating and understanding the important parameters that determine the dynamic response of the gun tube. These results can be compared with the critical velocity values obtained using finite element techniques. The finite element values will approach the exact solution as the mesh discretization increases.

Consider a thin orthotropic cylindrical shell of radius R subjected to a transient axisymmetric radial load (e.g., a moving internal pressure P). Figure 1 shows the geometry, coordinate system, and pressure loading condition being considered. The governing equation for this model with a moving internal pressure front, expressed as Heaviside step function, can be given by

$$m\frac{\partial^2 W}{\partial t^2} + D_x\frac{\partial^4 W}{\partial x^4} + \frac{12(1-v_{\theta x}v_{x\theta})}{h^2 R^2}D_\theta W = P(1-H(x-Vt)), \qquad (1)$$

2
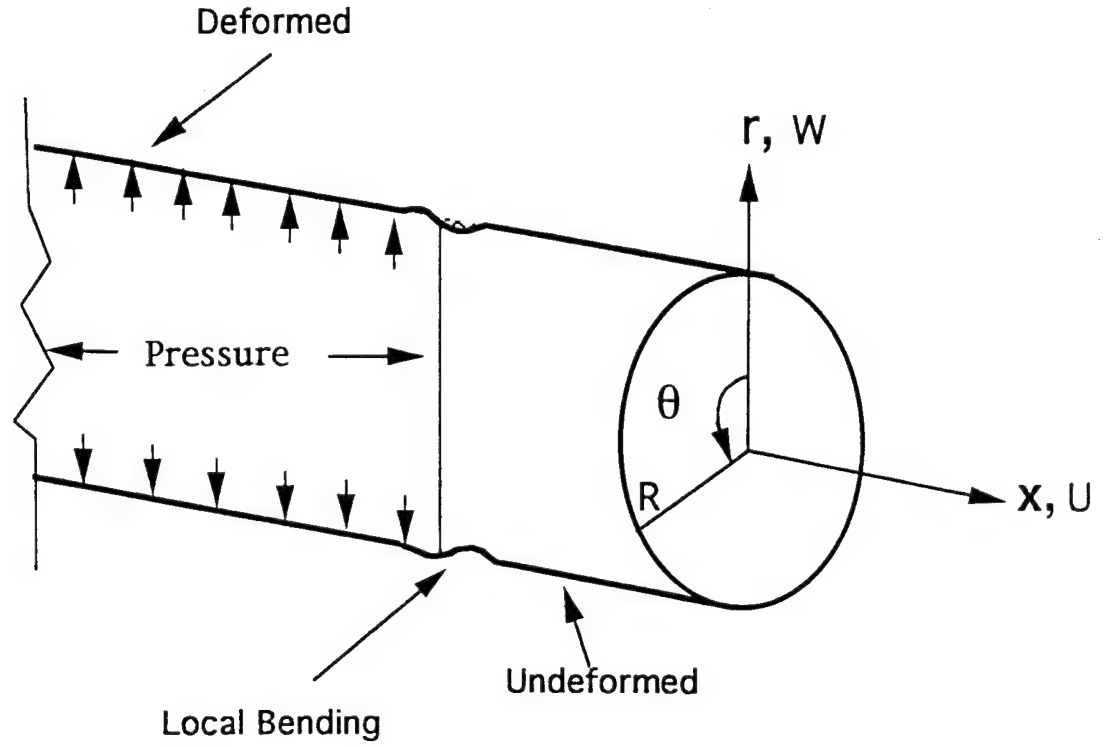
R: Radius of cylindrical shell

W: Radial displacement

U: Axial displacement

r, θ, x: Cylindrical coordinates

Figure 1. <u>Deformation and coordinates definition of cylindrical shell subjected to gun pressure.</u>

where W is the radial displacement, dependent upon time, t, and axial position coordinate, x, m is the mass which is equal to ρh, ρ is the density of shell material, h is the thickness of the shell, P is the internal pressure, and V is the pressure front velocity, which is constant. The shell bending stiffness in the axial and circumferential directions is given by the expressions in equation (2) and equation (3), respectively.

$$D_x = \frac{E_x h^3}{12(1 - \nu_{\theta x} \nu_{x\theta})} \qquad (2)$$

$$D_\theta = \frac{E_\theta h^3}{12(1 - \nu_{\theta x} \nu_{x\theta})}, \qquad (3)$$

3

where E_x and E_θ are the effective (smeared) elastic moduli, and $\nu_{x\theta}$ and $\nu_{\theta x}$ are the effective Poisson's ratios of the composite material in the axial and circumferential directions, respectively. For a composite tube with cross-ply laminate construction, the shell bending stiffness is different in the axial and circumferential directions and is determined by the axial-to-hoop layer ratio.

The loading function, $P(1 - H(x - Vt))$ in equation (1), represents the internal pressure front traveling in the axial direction with constant velocity V. $H(x - Vt)$ is the Heaviside step function. Accordingly,

$$P(1 - H(x - Vt)) = 0 \qquad \text{when} \quad x > Vt$$
$$= P \qquad \text{when} \quad x \leq Vt. \tag{4}$$

The critical velocity for an orthotropic cylindrical shell, derived from the characteristic function obtained from equation (1), is given by

$$V^2_{cr,comp} = \sqrt{\frac{1}{3\left(1 - \nu_{\theta x}\nu_{x\theta}\right)}} \left(\frac{h}{R}\right)\left(\frac{\sqrt{E_\theta E_x}}{\rho}\right). \tag{5}$$

Equation (5) clearly shows that the critical velocity of an orthotropic cylinder subjected to a moving pressure front is a function of the tube's thickness and radius, density, Poisson's ratios, and elastic moduli. The critical velocity increases when either of the elastic moduli increase as well as when the shell thickness-to-radius ratio increases. From a design point of view, a tube constructed with high stiffness and lightweight materials is preferred for dynamic loading conditions. However, equation (5) indicates that a larger wall thickness is required, in general, when a high-velocity pressure front is present. It also shows that both the hoop and axial moduli (e.g., $E_\theta = E_x$) have influence on the critical velocity. Accordingly, the desired tube design for the dynamic loading condition can be achieved by optimizing the laminate architecture of the composite overwrap.

For an isotropic cylinder, equation (1) reduces to

$$m\frac{\partial^2 W}{\partial t^2} + D\frac{\partial^4 W}{\partial x^4} + \frac{Eh}{R^2} W = P(1 - H(x - Vt)), \tag{6}$$

4

where D, the bending stiffness of the shell, is given by

$$D = \frac{Eh^3}{12(1-v^2)}.$$ (7)

The critical velocity at which resonance occurs in this isotropic tube is therefore given by

$$V^2_{cr,\,steel} = \sqrt{\frac{1}{3(1-v^2)}} \left(\frac{h}{R}\right)\left(\frac{E}{\rho}\right).$$ (8)

The critical velocity of an isotropic cylinder, equation (8), is thus seen to be very similar to the critical velocity of an orthotropic cylinder, equation (5). As discussed previously, it is important from a design point of view to be able to estimate the critical velocity of gun tubes constructed from various materials.

2.2 Finite Element Solution. The closed-form solution described in the previous section can be applied accurately to a cylindrical shell under the assumption of infinite length. For a finite length gun tube with varying cross-sectional area along its length and multi-material construction, the finite element method allows a more expedient and straightforward procedure for determining the critical velocity. DYNA2D, a hydrodynamic finite element code, was modified to simulate the moving pressure boundary condition. A schematic of the finite element modeling technique is shown in Figure 2. A slideline that allows a dummy projectile to move freely along the axial direction of the gun tube is included in a finite element model of the gun tube. The instantaneous location of the pressure front is then easily determined by tracking the location of the rear face of the dummy projectile. To accurately capture the oscillatory dynamic response of the tube, the computation is carried out with a very fine time interval ($\sim 10^{-6}$ s). This time interval also allows the pressure to slowly ramp to maximum value as element surfaces are uncovered by the moving projectile. This means that artificial numerical stress oscillations, due to the sudden application of the pressure boundary condition on an element face, are minimized such that these numerical oscillations do not adversely affect the solution. While the projectile velocity was held constant for the cases examined in this study, the methodology also can be used to simulate the effect of an accelerating projectile if desired.

5

Dummy Projectile

Pressure

Slidline
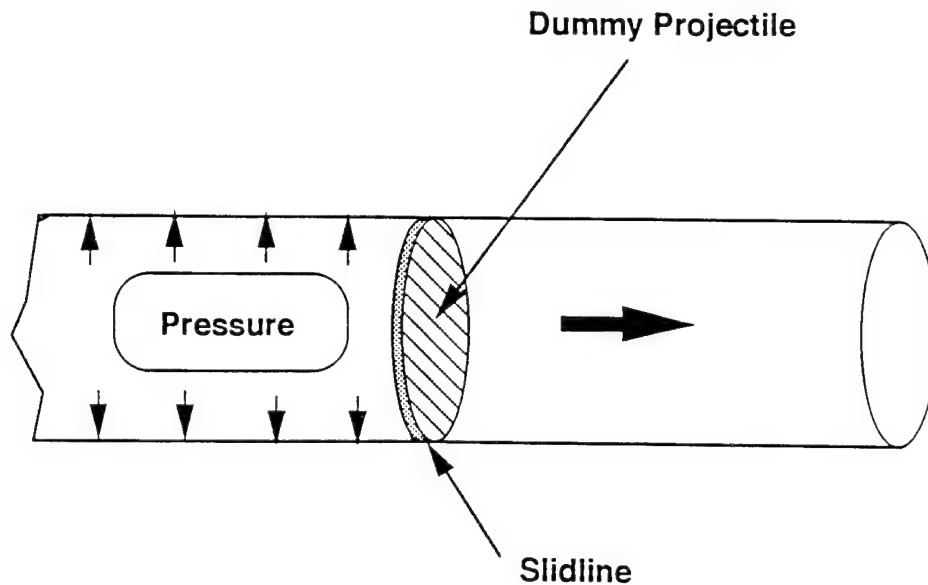
- Real time simulation of moving pressure
- Dynamic analysis
- Constant pressure

Figure 2. <u>A schematic of the finite element analysis.</u>

Since the composite tube has a laminated construction, ideally a ply-by-ply model will yield the best result and accuracy. However, this would dictate the use of many thousands of elements in the finite element model. This level of detail, coupled with the very short time step interval required for a dynamic analysis, would lead to an unreasonably long computational time. Also, an additional potential side effect of taking many millions of time steps would be to potentially induce numerical instabilities due to round-off errors. Avoiding these constraints thus limits the size (e.g., number of elements) of the finite element model that can be analyzed within a reasonable computational time. In composite analysis, it is standard practice to use smeared properties for the composite laminate. These properties, which represent the unique layup construction of the tube, were calculated using a model developed by Alexander et al. (1994). The smeared property approach allows a single finite element to contain several layers. Accordingly, the size of the finite element model can be greatly reduced. The smeared properties for a composite tube composed of 25% axial (x-direction) and 75% hoop (θ-direction) plies are shown in Figure 3. The properties are calculated based on the use of an IM7 graphite/8551-7 epoxy composite. The unit ply properties are also given in this figure.
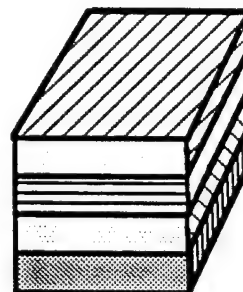
6
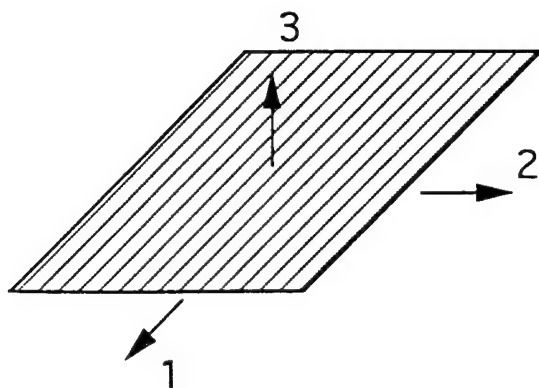
$E_{11} = 25.0E+06$ $\quad$ $G_{12} = 7.0E+05$

$E_{22} = 1.2 E+06$ $\quad$ $G_{13} = 7.0E+05$

$E_{33} = 1.2 E+06$ $\quad$ $G_{23} = 5.3E+05$

$\nu_{12} = 0.33$ $\quad\quad$ $\nu_{23} = 0.31$

$\nu_{13} = 0.33$
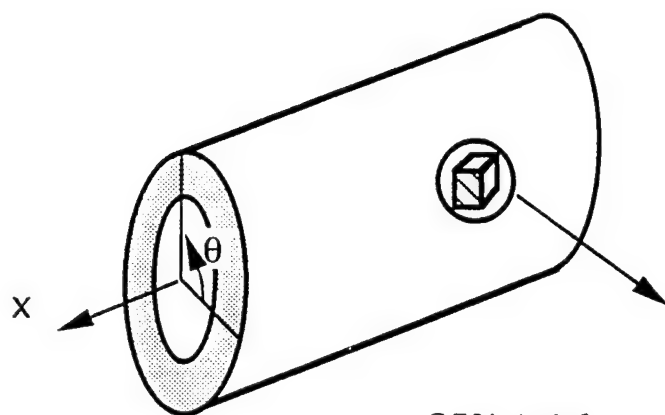
25% Axial
75% Hoop

$E_r = 1.298E+06$ $\quad$ $G_{rx} = 4.095E+05$

$E_x = 7.214E+06$ $\quad$ $G_{\theta r} = 4.610E+05$

$E_\theta = 19.10E+06$ $\quad$ $G_{\theta x} = 7.000E+05$

$\nu_{\theta r} = 0.3825$ $\quad\quad$ $\nu_{xr} = 0.338$

$\nu_{\theta x} = 0.0556$

Figure 3. Smeared properties of the composite tube.

7

The geometry and other simulation parameters for the gun tube muzzle, which is typically the most critical region for dynamic strain amplification effects, are illustrated in Figure 4. The cylinder used in this analysis is 100 in long with a constant wall thickness representative of the muzzle geometry. The cylinder is equally divided into 200 elements along the axial direction. There are six elements through the thickness. These elements are divided into two elements representing the steel liner and four elements representing the composite overwrap. In all, this model uses 1,200 elements. The finite element analysis was performed for two designs in which the thickness of steel liner and composite overwrap were changed while still maintaining the same overall wall thickness. Design 2, which used a thicker steel liner, is a modification of Design 1. The muzzle pressure of 5,870 psi was determined using an interior ballistic pressure analysis. Two projectile muzzle velocities were considered. These muzzle velocities were a subcritical velocity of 2,500 ft/s (Case 1) and supercritical velocity of 3,430 ft/s (Case 2).

The total time for the projectile to traverse the tube was 3.33 ms and 2.43 ms for Cases 1 and 2, respectively. The time increment used in the analysis was on the order of 1 µs; therefore, approximately 3,500–4,000 time steps were used per analysis. The finite element model including the composite cylinder and the projectile is shown in Figures 5 and 6 at two different instants in time. Finally, because an axisymmetric model was employed, only one-half of the cylinder is shown. In Figure 5, the dummy projectile is shown at its initial position. The projectile is then given an initial velocity, which is held constant throughout the analysis. Figure 6 shows the projectile when it has traveled 20 in from the initial position. A fringe plot of the radial displacement in the neighborhood of the projectile at this specific instant is shown in Figure 7. The fringe pattern clearly shows the stress oscillation due to induced bending boundary layer stresses in the wall of the cylinder as it is subjected to a moving pressure front. The maximum displacement is located very close to the base of projectile. This corresponds to the location of the pressure loading discontinuity. The displacement then decreases with increasing axial distance from the location of the pressure front discontinuity. The deformation is transient and cyclic with time and position.

The previous way of presenting the data clearly shows the spatial variation of the displacement and, consequently, strain and stress fields. This view corresponds to what an observer traveling with the projectile as it traverses the gun tube would observe. An alternative view is to pick a fixed location on the tube and observe the change in displacement as the projectile approaches this position and then passes it (e.g., a time history plot for a given location). This corresponds to what is measured with strain gauges or accelerometers attached to the tube. Figure 8 shows the radial locations where various displacement
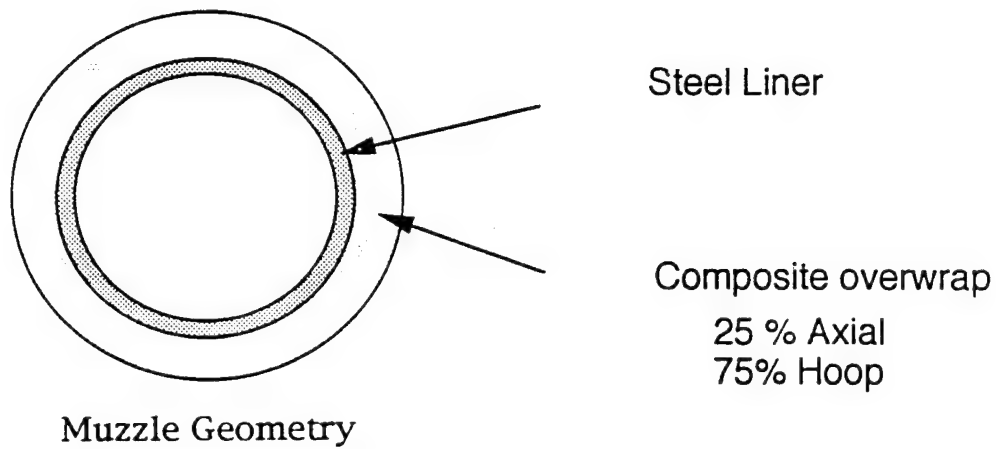
8

Figure 4. Muzzle geometry and design parameters.

Cylinder-modified v=3500 ft/sec
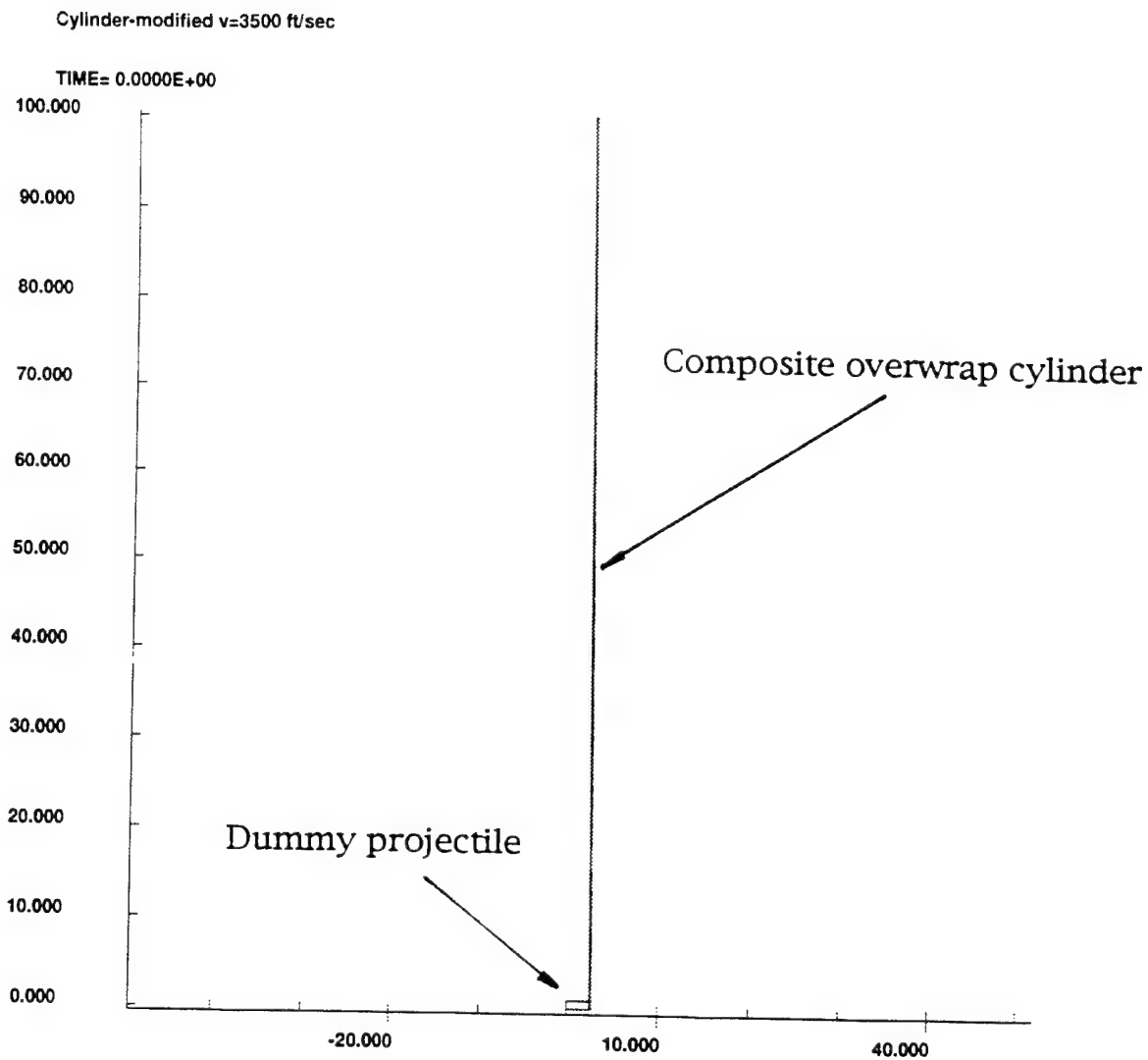
TIME= 0.0000E+00

Composite overwrap cylinder

Dummy projectile

Figure 5. Finite element model of the overwrapped composite cylinder with the dummy projectile at the initial position (time = 0.0 s).
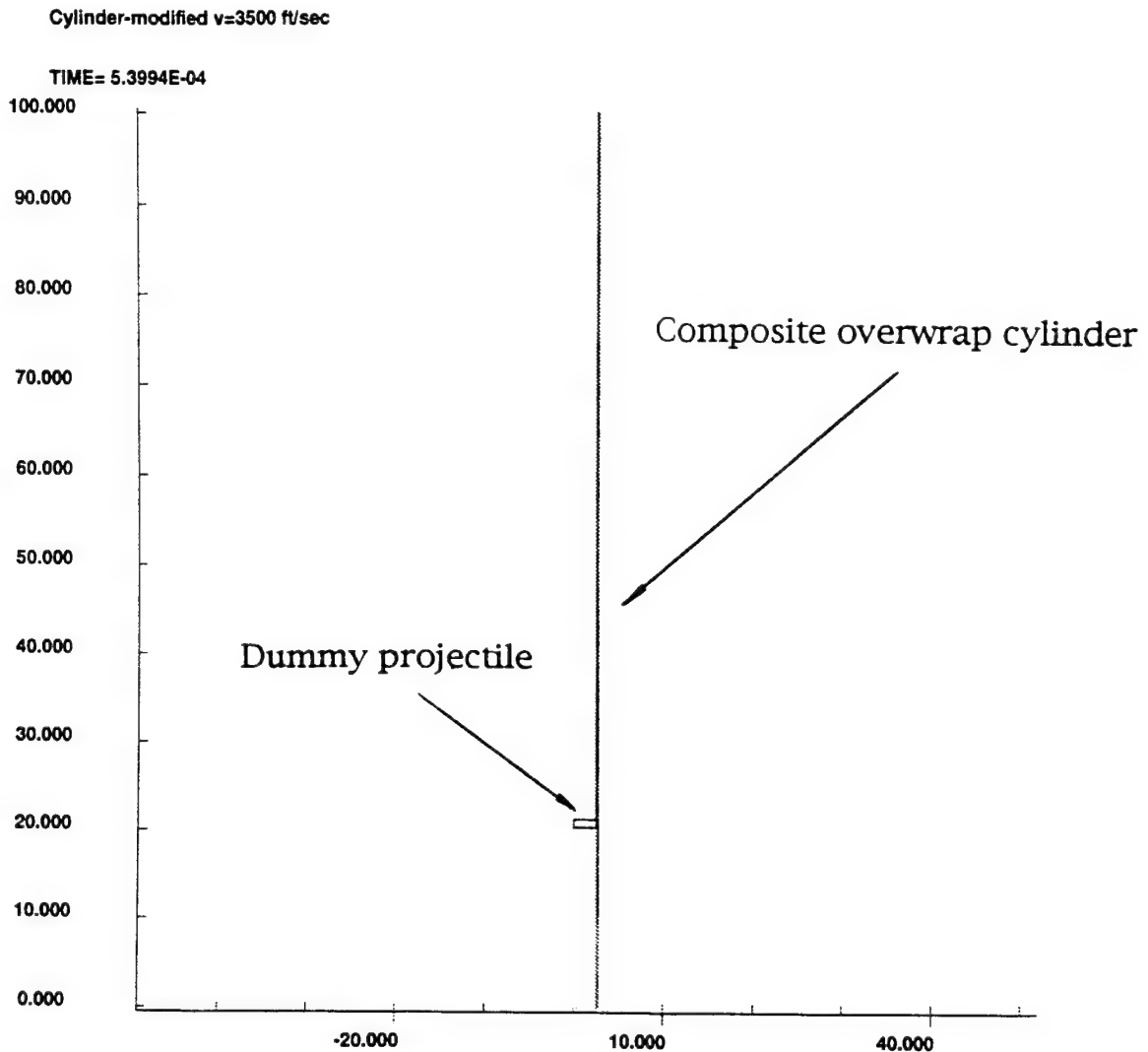
10

Cylinder-modified v=3500 ft/sec

TIME= 5.3994E-04

Composite overwrap cylinder

Dummy projectile

Figure 6. <u>Finite element model of the overwrapped composite cylinder with the dummy projectile at time = 5.3994E-4 s.</u>

and stress components are examined in this report. These radial locations represent positions at which displacement and stress components attain their greatest values. Since the tube is subjected to an internal pressure, the maximum hoop stress occurs at the inner surface of the liner. As the pressure front passes a given axial location, a local axisymmetric bending occurs in the wall of tube. The maximum axial stress will thus occur at the innermost surface of the liner and the outermost surface of the composite. The maximum shear stress associated with this bending is located at the neutral axis of the cross section. Accordingly, the critical value of the shear stress in the transverse direction of composite laminate occurs near the interface of the liner and the composite overwrap.
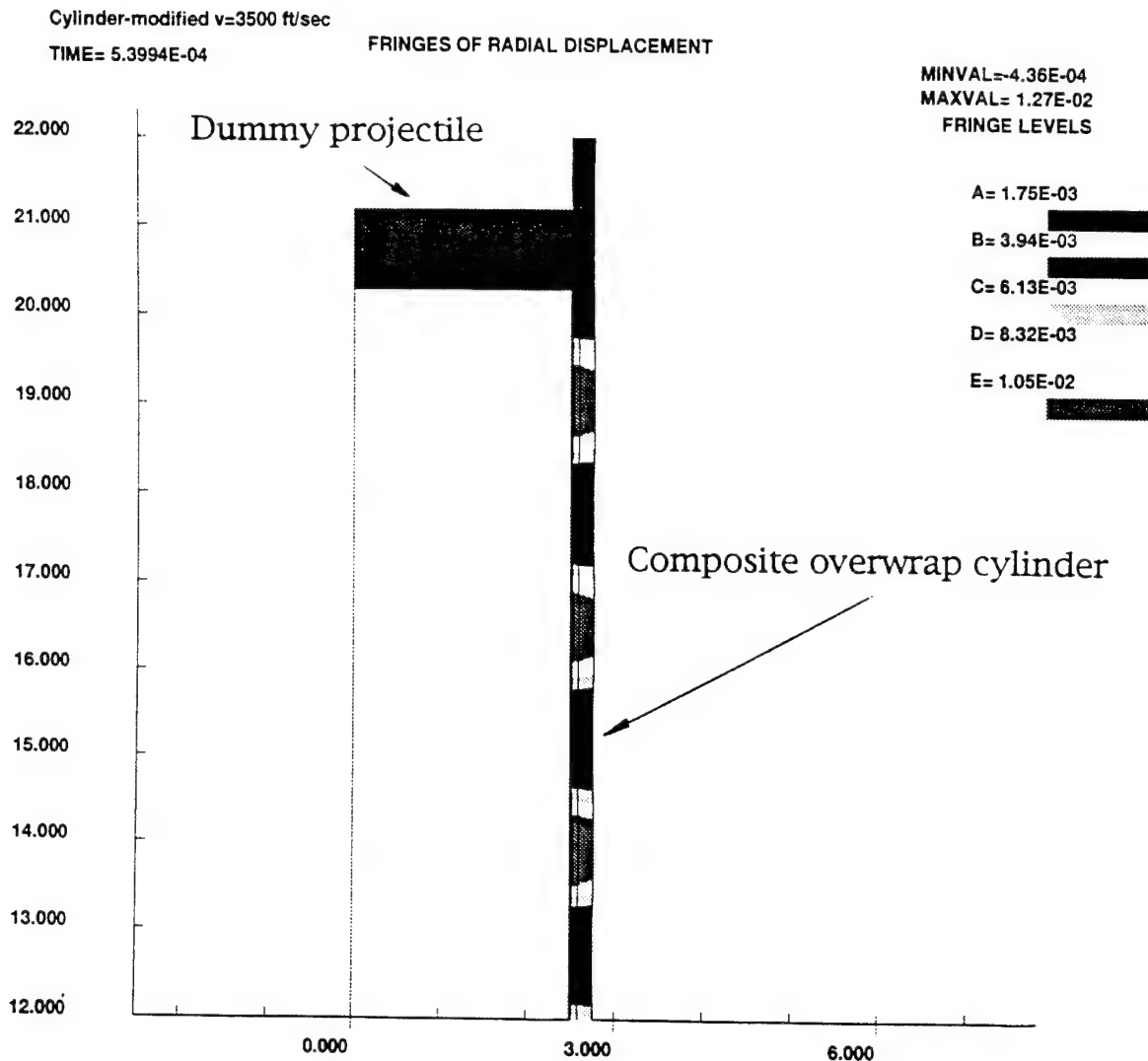
11

Figure 7. Radial displacement in the vicinity of the projectile passage at time = 5.3994E-4 s.

Figures 9–14 plot the various displacement and stress components vs. time at these locations for the cylinder of Design 1. The radial displacement at the innermost region of the composite (Figure 9) shows a dramatic difference in the magnitude of peak displacement as well as in temporal behavior of the oscillations as the projectile velocity changes, Case 1 vs. Case 2. Prior to the projectile arriving, the cylinder at these observed locations is basically undeformed. The small oscillations that occur just before projectile arrival are real and represent stress oscillations due the moving pressure front. Similar behavior is predicted by thin wall shell theory. It is seen that, at the instant the projectile passes, the radial displacement undergoes a rapid increase. However, for sufficiently low velocities, similar to Case 1, the displacements and stresses are still close to what would be predicted based upon Lamé's equations for a
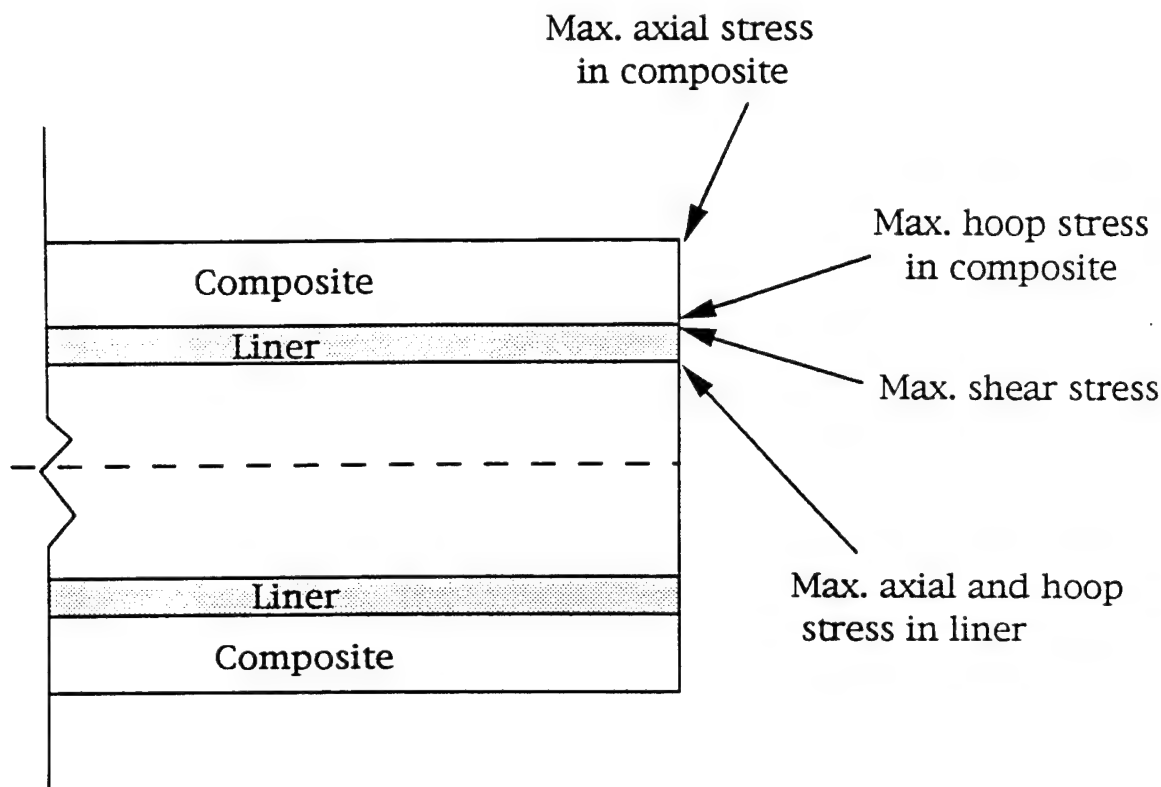
Figure 8. Locations of the maximum stress components.

static internal pressure loading. This is not the case though for velocities near or above the critical velocity shown in Figure 9, Case 2. A very large radial displacement occurs for this case where the projectile velocity is 3,430 ft/s. In fact, this velocity exceeds the critical velocity of the overwrapped composite cylinder. The peak magnitude of the radial displacement is seen to be about 1.5 times the peak magnitude of the radial displacement of Case 1 where the velocity is only 2,500 ft/s. As the projectile moves further away from this axial location, the radial displacement approaches the same magnitude ($\sim$7.5 $\times$ 10^{-3} in) as would be predicted by a static analysis of a pressurized tube. This is shown to be true for both Case 1 and Case 2. It is very important to realize that because the velocity for Case 2 is above the critical velocity, the peak radial displacement value is actually less than the peak value that would be obtained if the projectile had accelerated from 2,500 ft/s to 3,430 ft/s since, in this scenario, the projectile would have passed through the critical velocity at some axial location. This would have resulted in a resonant condition at that location, and the peak radial displacement would have been at least twice the Lamé prediction. In fact, theoretically, for linear elastic behavior, the response would have been infinite. This means that the material response would have been limited only by the internal damping of the material coupled with its behavior after yield.
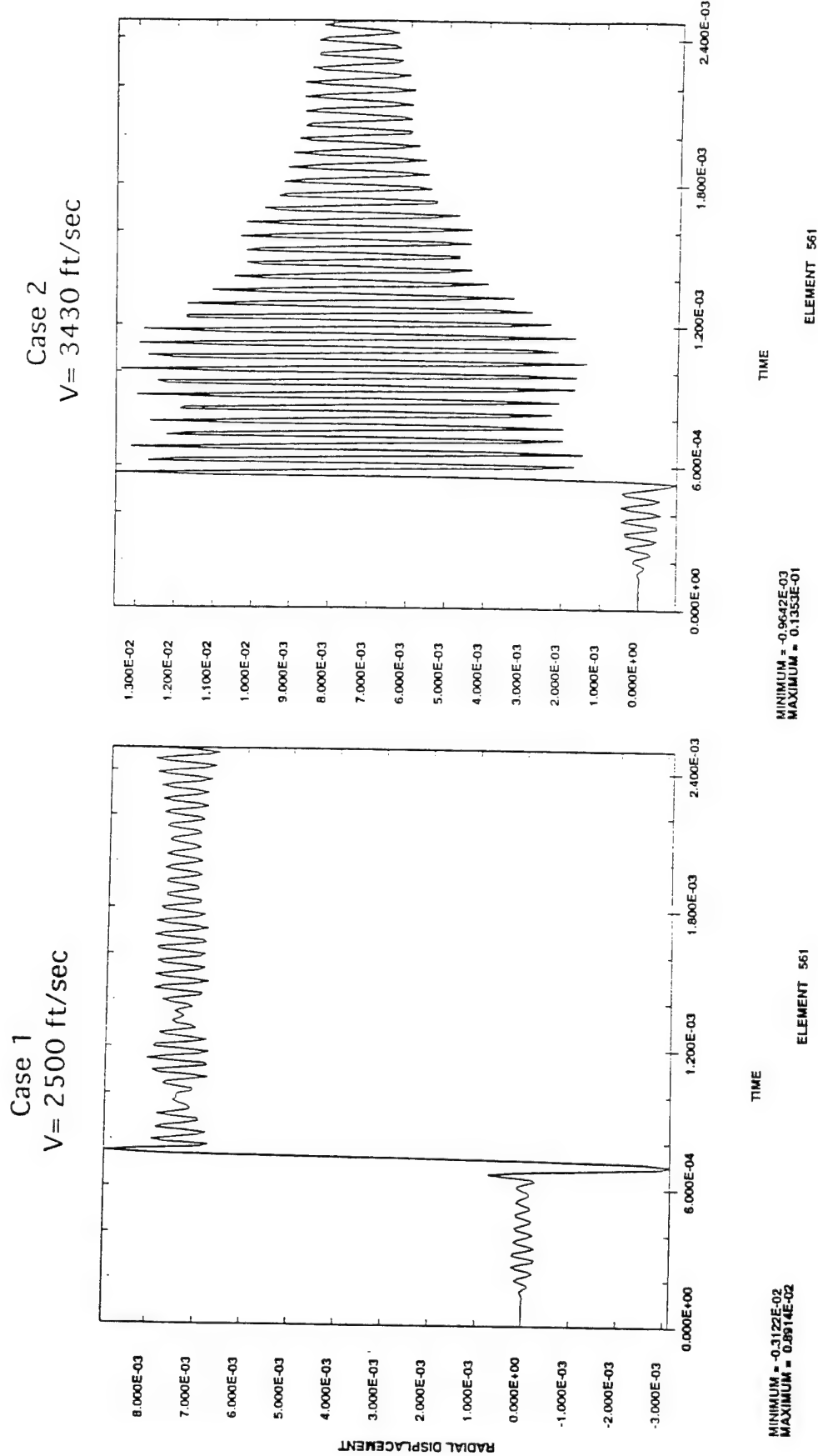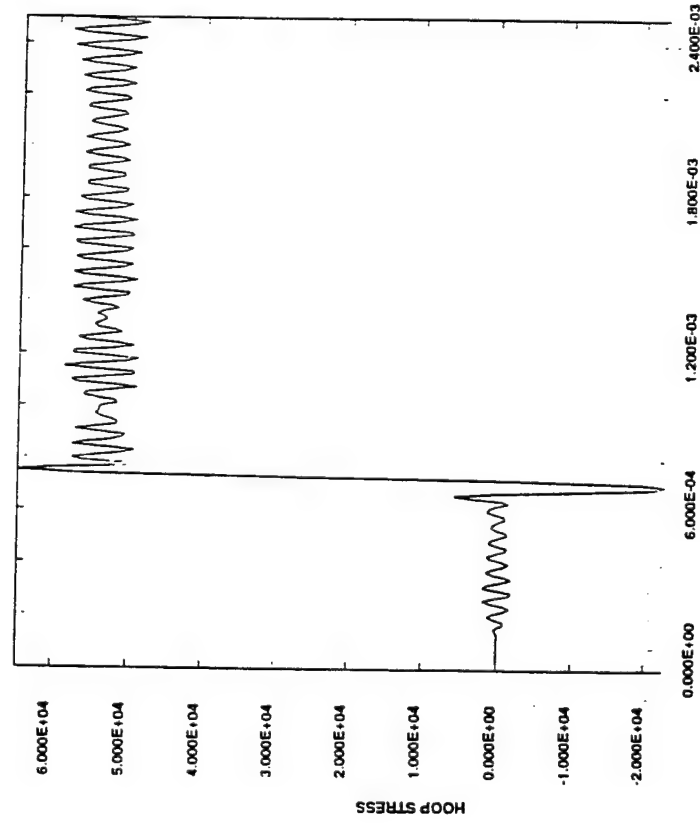
Figure 9. Radial displacement in the innermost region of the composite overwrap of Design 1.

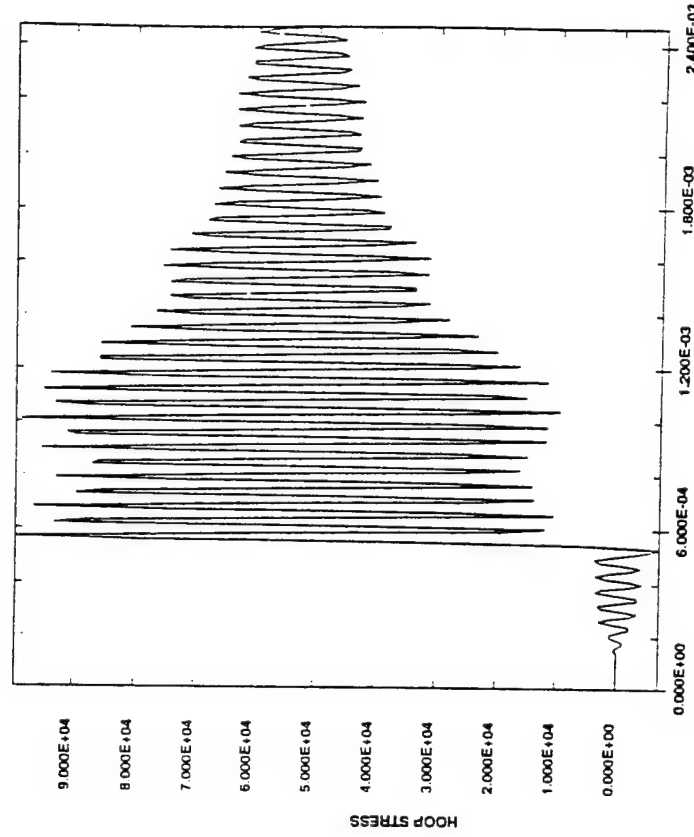Figure 10. Hoop stress in the innermost region of the composite overwrap of Design 1.

15
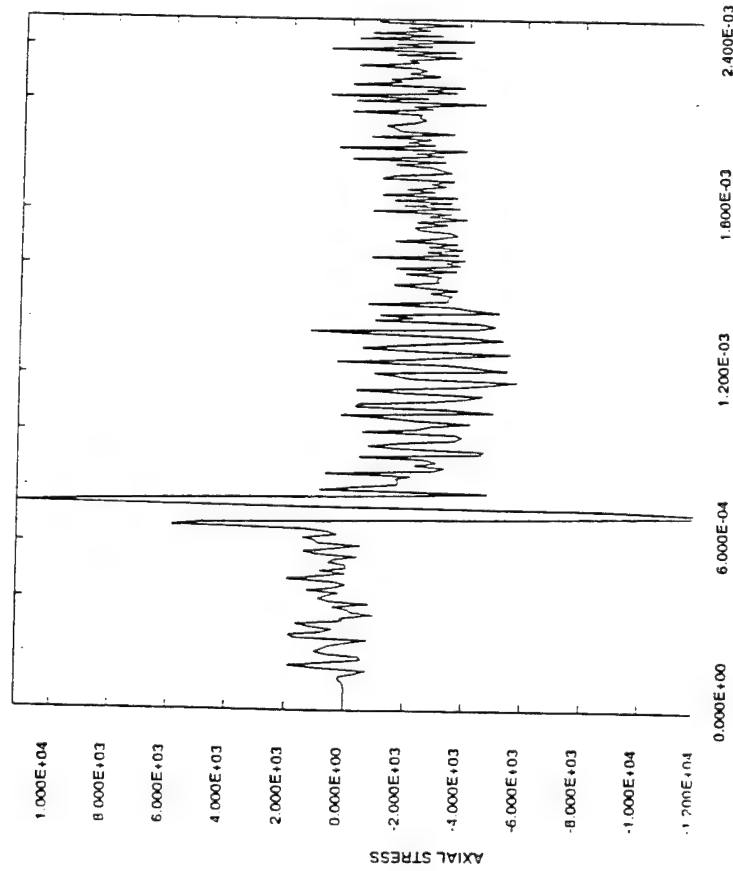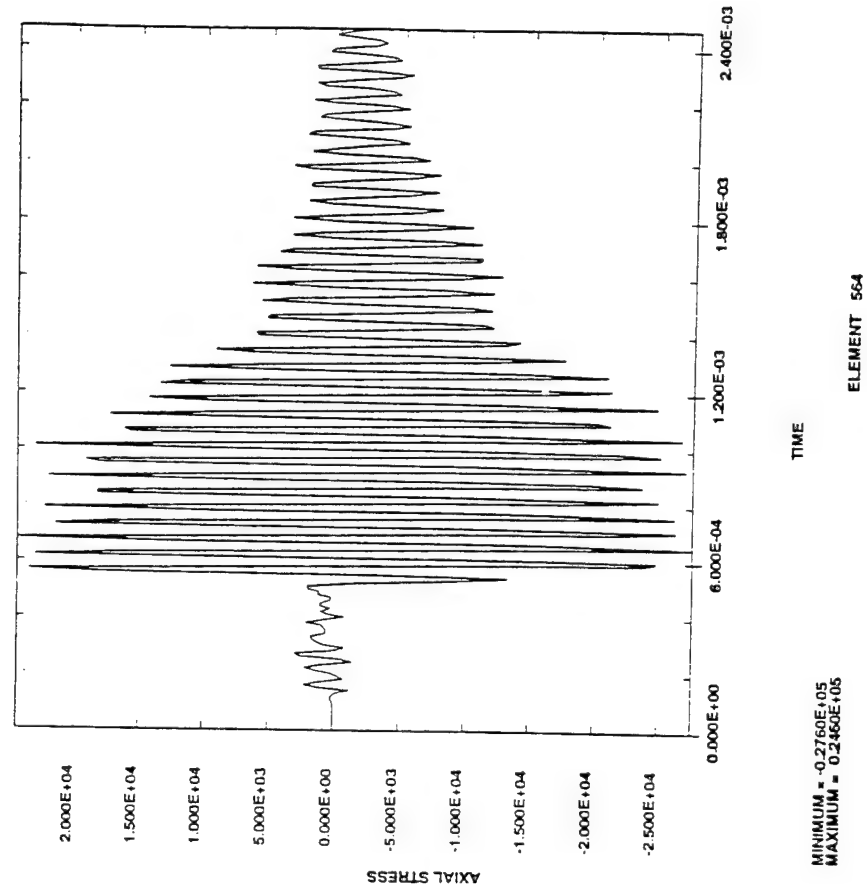
Figure 11. Axial stress in the outermost region of the composite overwrap of Design 1.
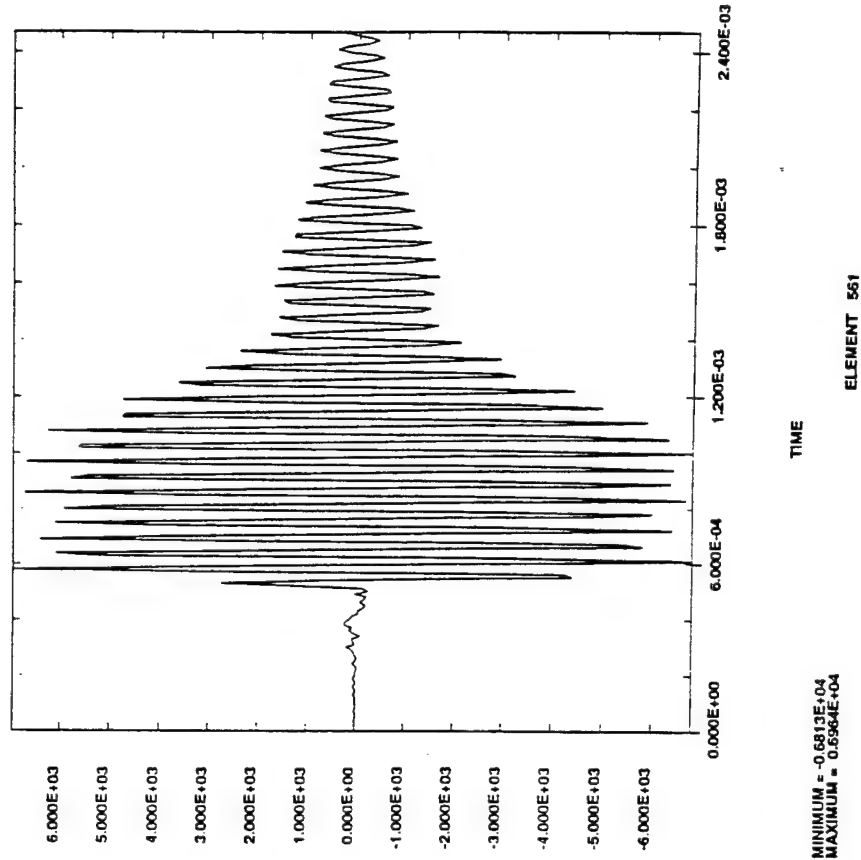
16
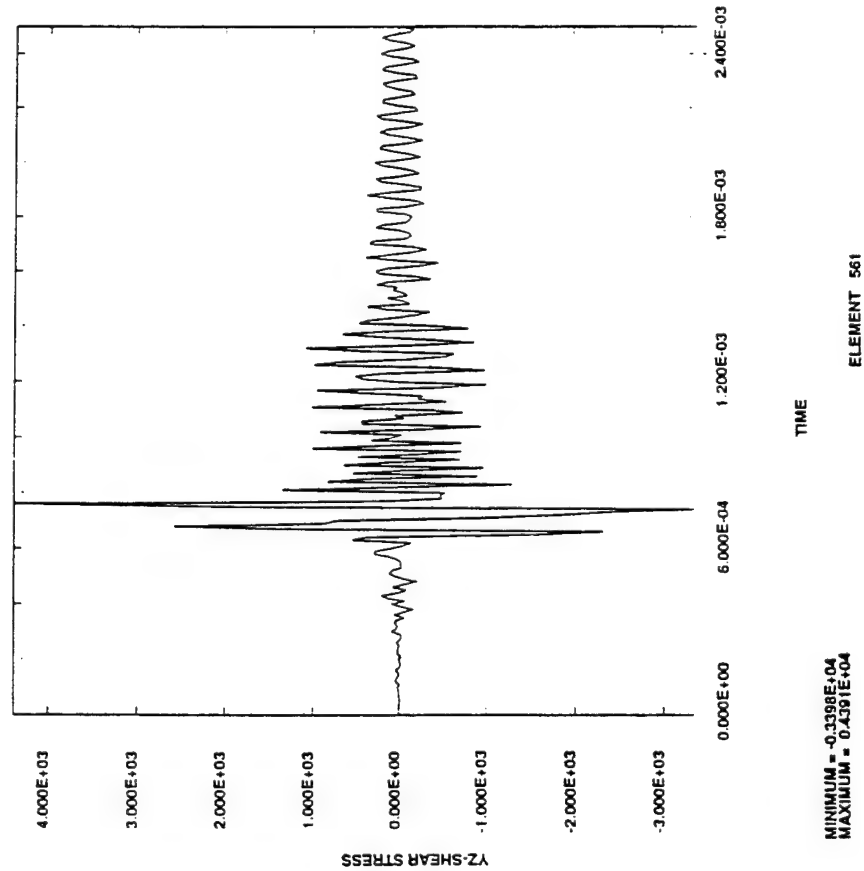
Figure 12. Interlaminate shear stress in the innermost region of the composite overwrap of Design 1.

17
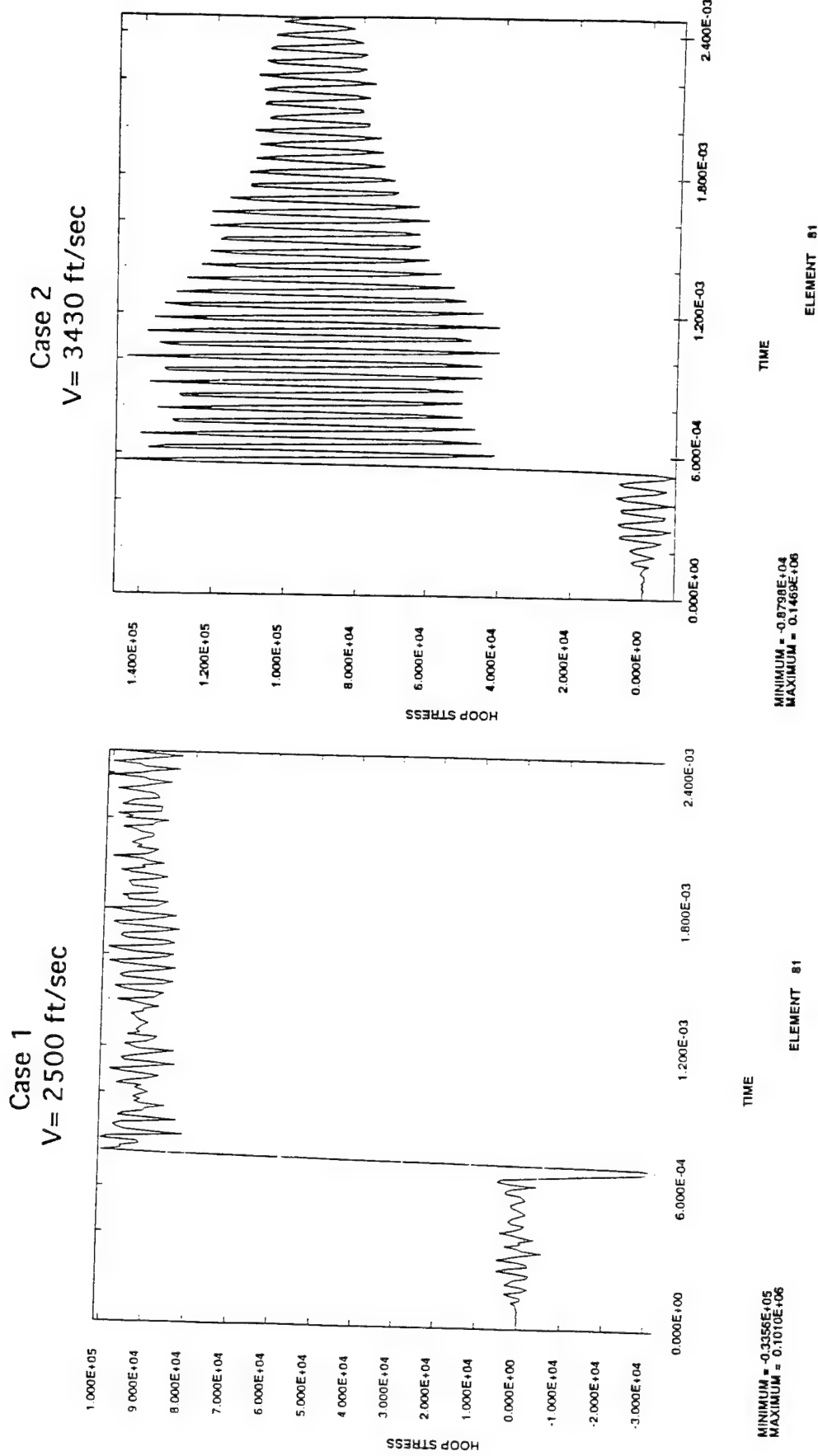
Figure 13. Hoop stress in the innermost region of the steel liner of Design 1.
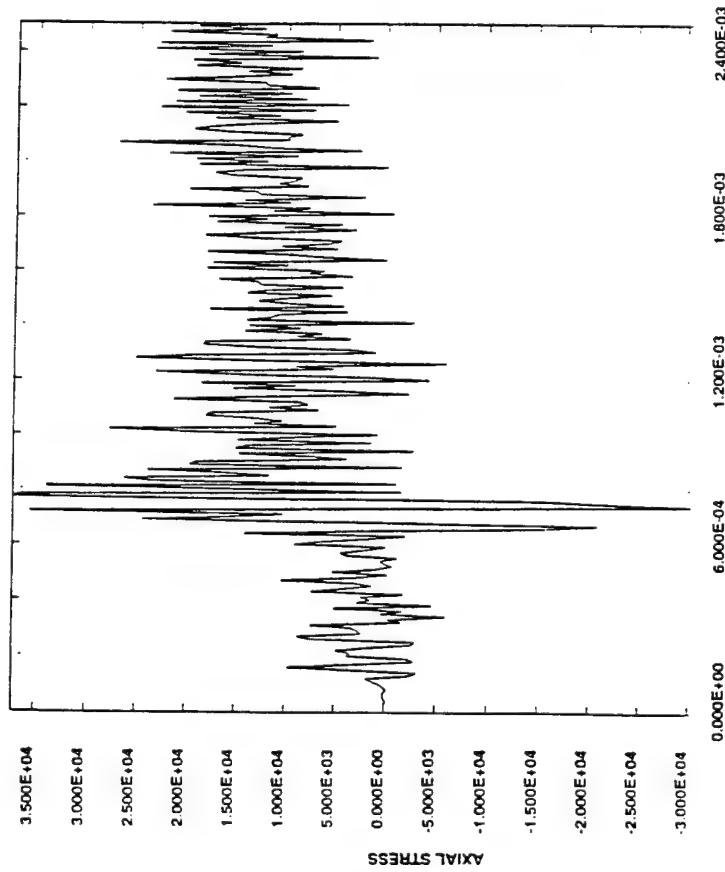
18

Figure 14. Axial stress in the innermost region of the steel liner of Design 1.

19

Figure 10 shows the smeared hoop stress induced at the innermost composite region. The composite overwrap is constructed with 75% hoop and 25% axial plies, and the smeared hoop stress is, in some sense, the average value for a small representative volume of the laminate at this location. A simple rule-of-mixtures calculation indicates that the peak unsmeared fiber stress in the hoop direction is about 86 ksi for the low-velocity case and 135 ksi for the high-velocity case. The effect of resonance due to a fast-moving pressure front is again clearly indicated. Figure 11 shows the smeared axial stress at the outermost radius of composite overwrap. The computed fiber stress is approximately 45 ksi and 100 ksi for the low- and high-velocity cases, respectively. Again, this is based on a simple rule-of-mixtures approach. Figure 12 shows the σ_{rz} shear stress at the innermost radius of composite overwrap, which is near the neutral axis of the combined steel/composite tube. The σ_{rz} shear stress is in the transverse direction of the laminate. The stress levels are 4.3 ksi and 7.0 ksi for the low- and high-velocity cases, respectively. Considering manufacturing factors and the low adhesion strength at the steel/composite interface, the 7.0-ksi shear stress indicates a low margin of safety factor.

Figures 13 and 14 show the hoop and axial stresses, respectively, at the innermost radius of the liner. Both the hoop and axial stresses show the resonance effect for the case of high velocity. These high-frequency stress oscillations may not cause immediate failure of the liner since the peak magnitude is below the failure stress of high-quality steel, although the comments on the effect of an accelerating projectile as discussed previously must be kept in mind. However, of potential importance is the effect of these high-frequency stress oscillations on the fatigue behavior of the gun and the effect this may have in reducing the life-cycle of the gun tube due to fatigue of either the liner or composite overwrap materials.

Based on these results, a second design was proposed with the intent of reducing the stress levels induced in the steel and composite overwrap by the dynamic strain amplification effect. The thickness of the steel liner was increased, while the total wall thickness was maintained constant. The objective of this design was to increase the stiffness in the axial direction and carry more load with the steel liner. The finite element model results for Design 2 are presented in Figures 15–20.

In general, the overall levels of stress and strain for Design 2, for both low- and high-velocity cases, are much lower than those of Design 1. In particular, the interlaminate shear is reduced to 5.80 ksi. This is to be compared with the value of 7.0 ksi for the high-velocity case for Design 1. The increase of the liner thickness shifts the neutral axis of the tube closer to the steel liner. Accordingly, more shear load

20
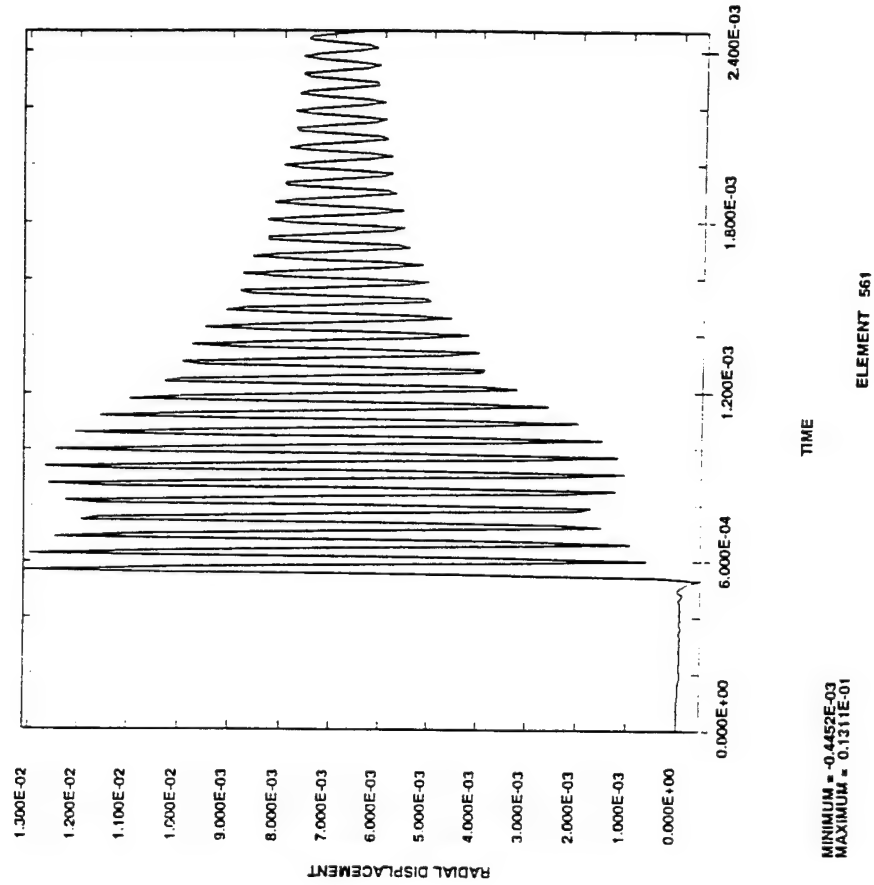
Figure 15. Radial displacement in the innermost region of composite overwrap of Design 2.

21

Case 2
V= 3430 ft/sec
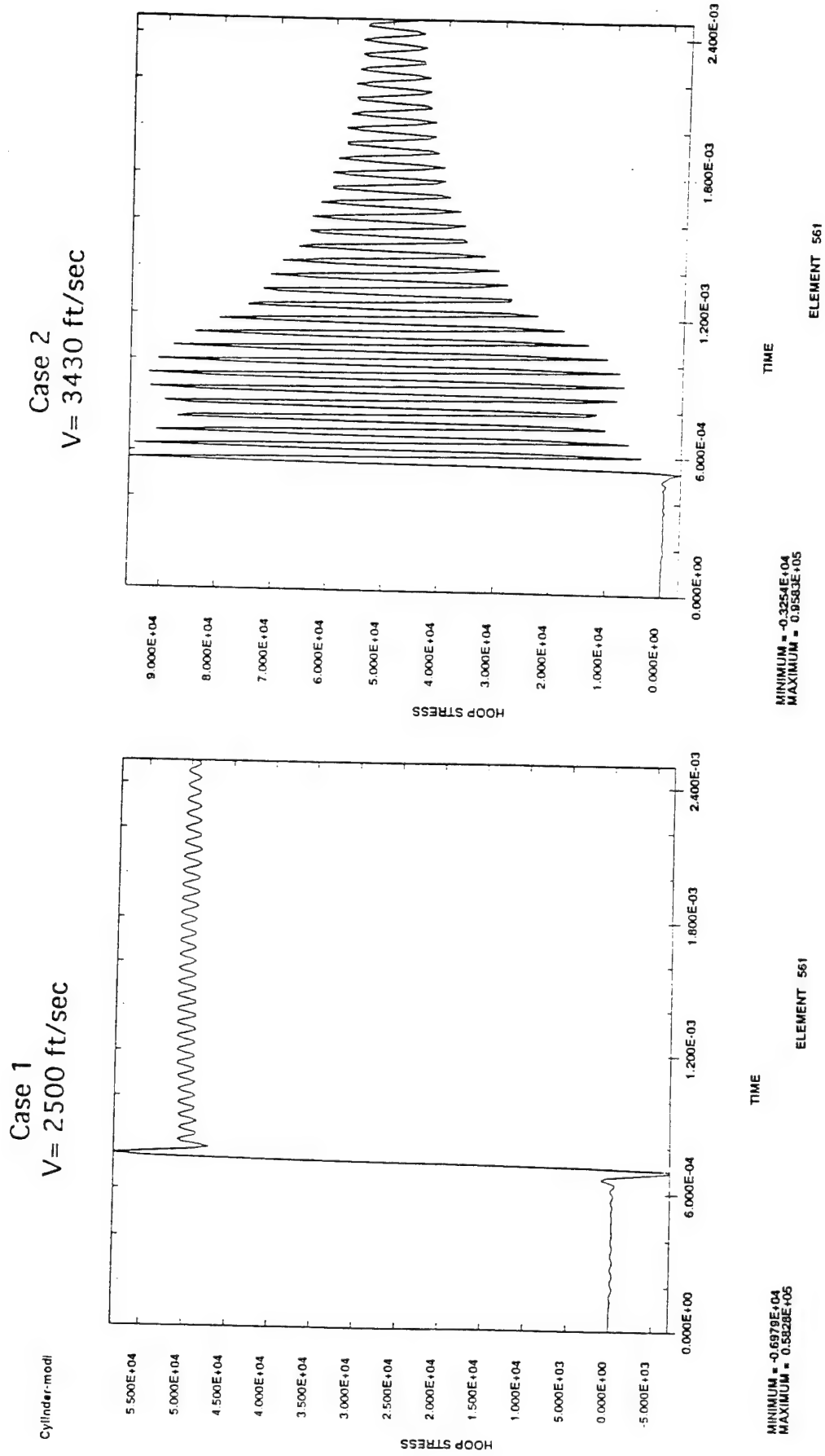
Case 1
V= 2500 ft/sec

Figure 16. Hoop stress in the innermost region of the composite overwrap of Design 2.

22

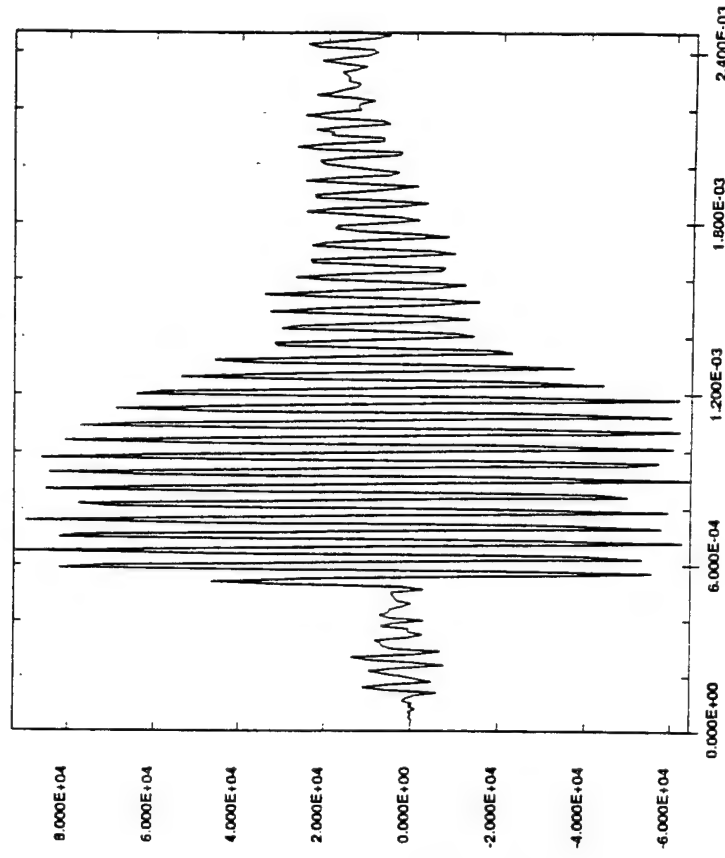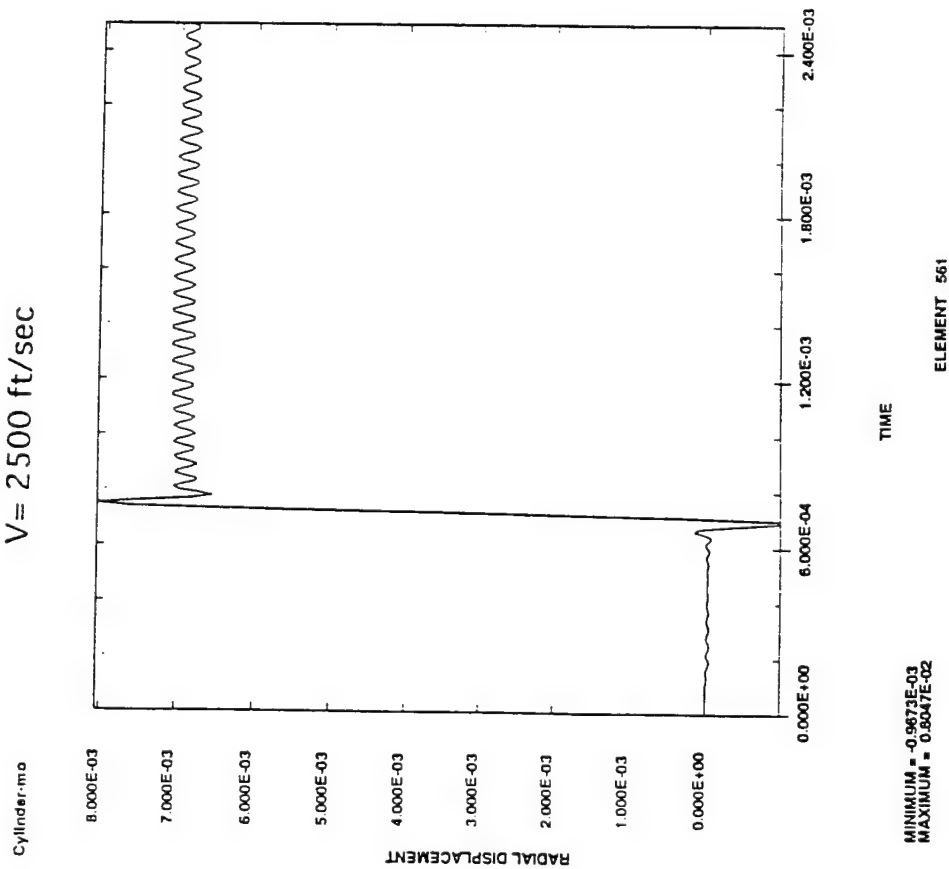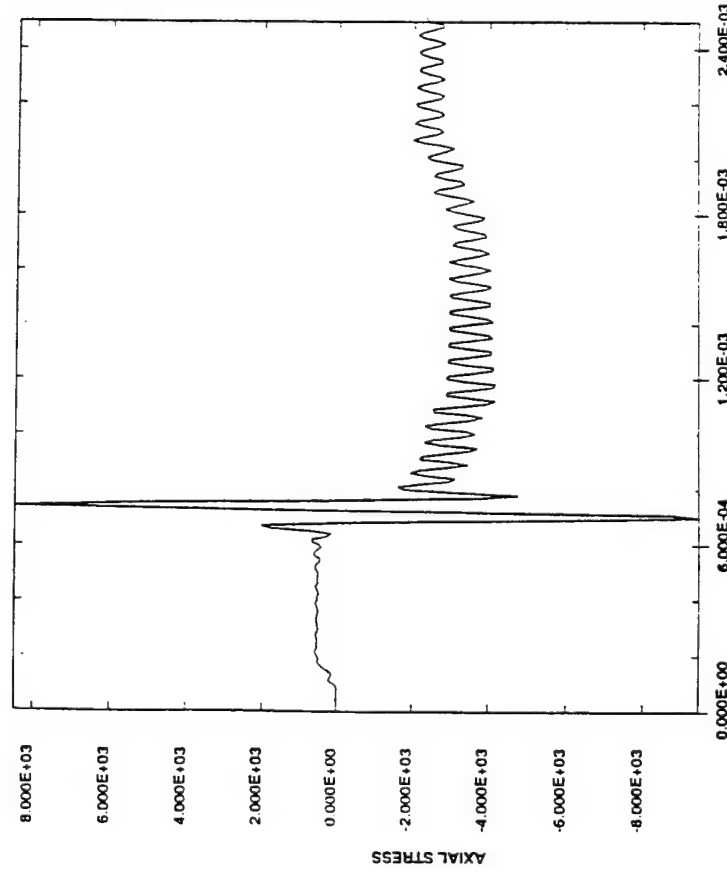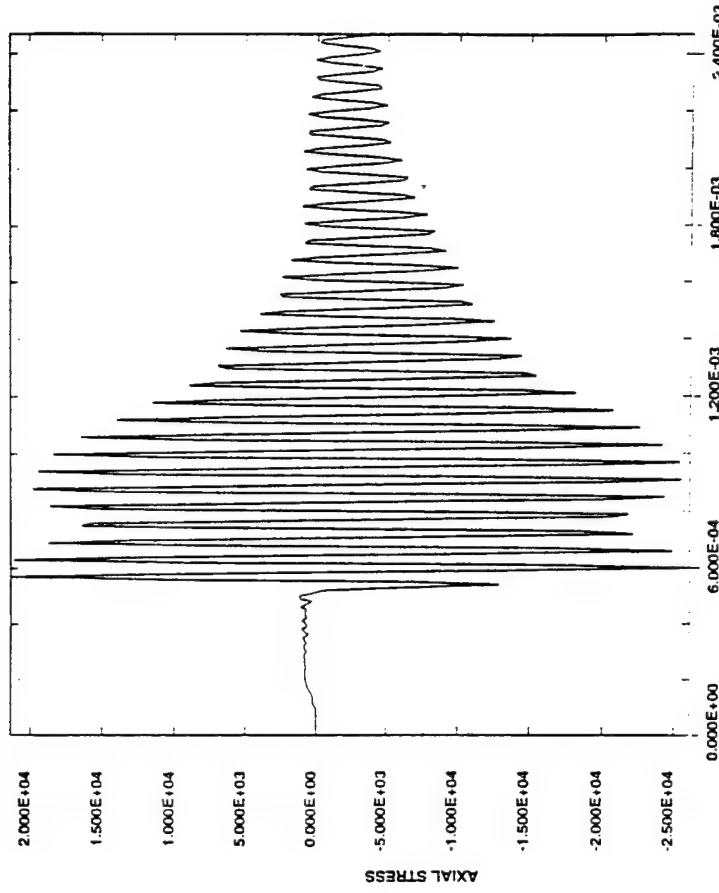Figure 17. Axial stress in the outermost region of the composite overwrap of Design 2.

23
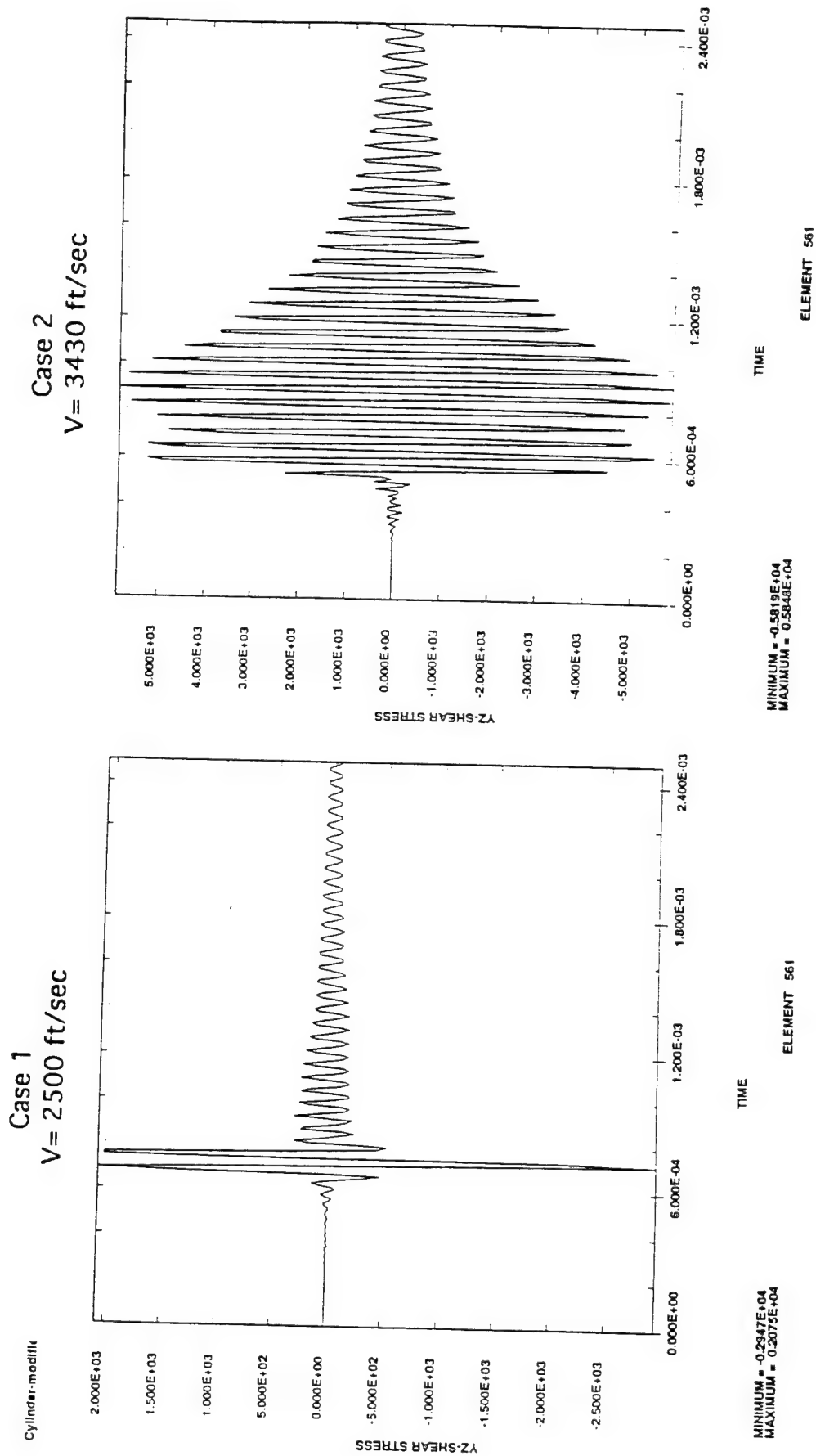
Figure 18. Interlaminate shear stress in the innermost region of the composite overwrap of Design 2.

24

Case 1
V= 2500 ft/sec

Cylinder-ma

ELEMENT 81

TIME

MINIMUM = -0.7905E+04
MAXIMUM = 0.9466E+05

Case 2
V= 3430 ft/sec

ELEMENT 81

TIME

MINIMUM = -0.1675E+04
MAXIMUM = 0.1430E+06
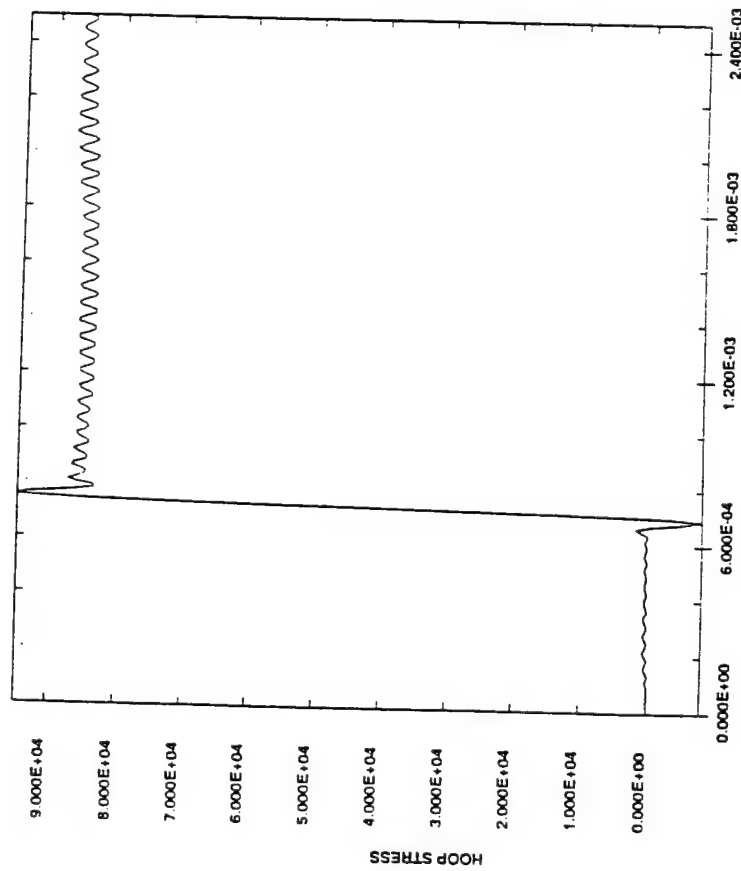
Figure 19. Hoop stress in the innermost region of the steel liner of Design 2.

25

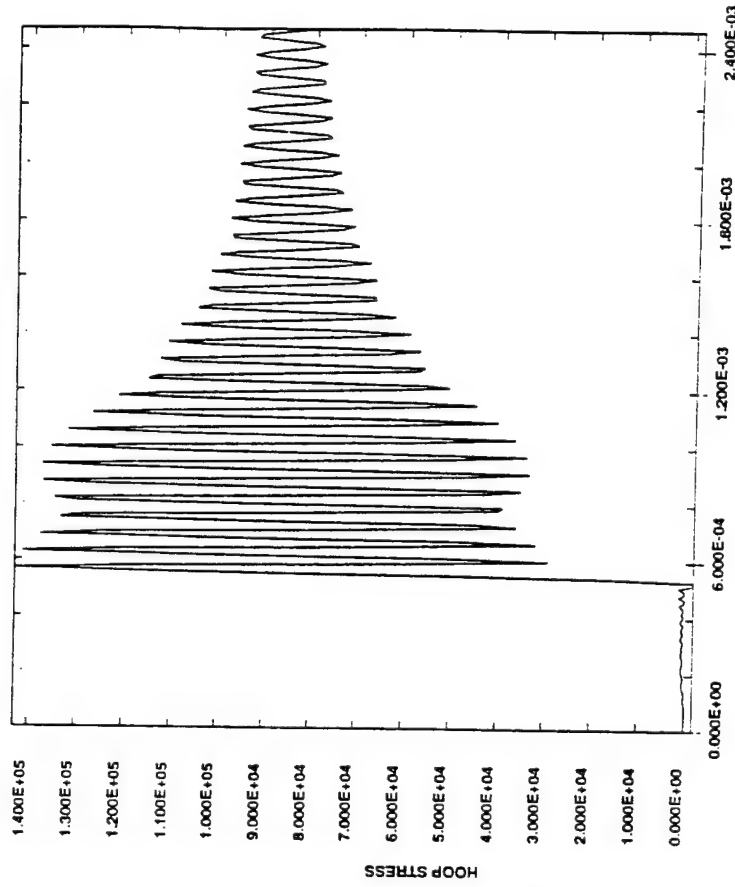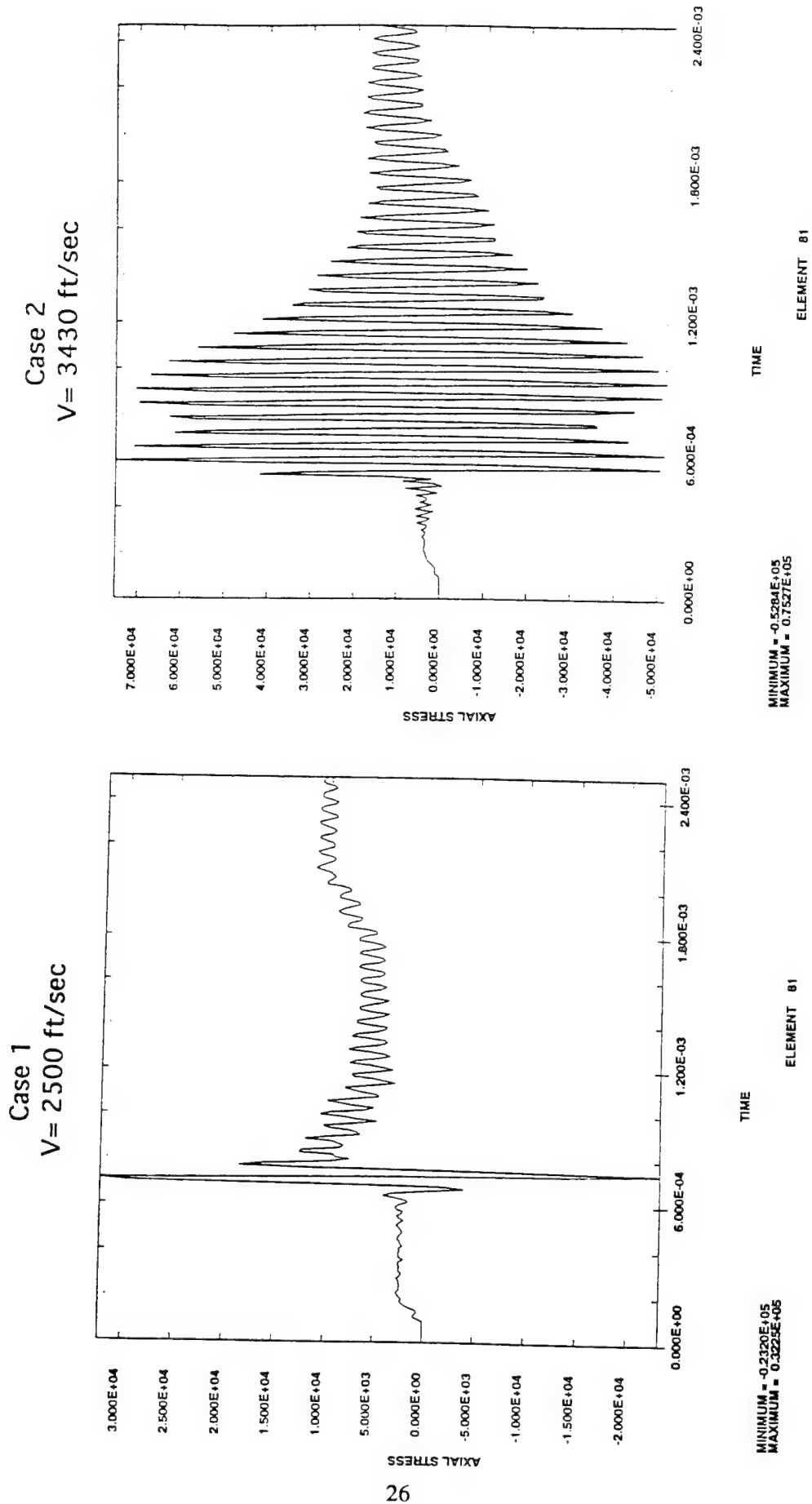Figure 20. Axial stress in the innermost region of the steel liner of Design 2.

26

is carried by the liner as opposed to the composite overwrap. The peak axial stress in the steel liner is 75.0 ksi for Design 2, which is less than the 93.0-ksi value predicted for Design 1 for the high-projectile velocity case. This reduction is due in part to the increase in the area moment of inertia of the thicker steel liner.

The use of a thicker steel liner also leads to a different value for the critical velocity. However, for both design configurations, the critical velocity is less than 3,430 ft/s according to the finite element analysis. It is possible to estimate the critical velocity approximately using the thin-shell solution derived previously. The difference of the smeared modulus-to-density ratio is 5% for these two designs using a rule-of-mixture analysis. The critical velocity is proportional to the modulus-to-density ratio. It is expected that the difference of the critical velocity is of approximately the same percentage change. Accordingly, it is not expected that the overall dynamic response will change dramatically due to this small design change.

3. CONCLUSIONS

The dynamic analysis of an overwrapped composite tube illustrates that high magnitude strains and stresses develop in the tube at the rear face of the projectile as the projectile traverses the length of the tube. The high magnitudes, commonly referred to as dynamic strain amplification, are caused by a resonance condition of the flexural wave propagation with the moving pressure front velocity. These results are important in highlighting the potential shortcomings of traditional static analysis commonly used in gun tube design. This dynamic strain effect can potentially cause damage and lead to a shortened life-cycle of the gun tube. The dynamic effect is particularly critical for the lightweight overwrapped composite gun barrels because of the low shear stress strength at the composite and the interface of multi-material construction and the potential of thermal degradation of polymer composite materials to further reduce these strength levels. To arrive at a safe, optimum design, the dynamic effect must be included. However, the unique laminated construction of composite materials also provide a great potential in design optimization. The desired tube design for dynamic loading conditions can be achieved by choosing proper layup and stacking sequence of laminates. This report illustrates one approach to analyzing proposed designs using finite element methods and including the effect of a moving pressure front.

27

INTENTIONALLY LEFT BLANK.

4. REFERENCES

Taylor, G. I. "Strains in a Gun Barrel Near the Driving Barrel of a Moving Projectile." A. C. 1851/Gn. 104, U.K. Ministry of Supply, London, England, March 1942.

Jones, J. P., and P. G. Bhuta. "Response of Cylindrical Shell to Moving Loads." Journal of Applied Mechanics, vol. 31, Trans, ASME, vol. 86, Series E, pp. 105–111, March 1964.

Tang, S. "Dynamic Response of a Tube Under Moving Pressure." Journal of the Engineering Mechanics Division Proceedings of the ASCE, pp. 97–122, October 1965.

Reismann, H. "Response of a Prestressed Cylindrical Shell to Moving Pressure Load, Development in Mechanics." Solid Mechanics - Proceedings of the Eighth Midwestern Mechanics Conference, Pergamon Press, Part II, vol. 2, pp. 349–363, 1965.

Simkins, T. E. "Response of Flexural Waves in Gun Tubes." ARCCB-TR-87008, U.S. Army Armament Research, Development, and Engineering Center (ARDEC), Benet Weapons Laboratory, Watervliet, NY, July 1987.

Hopkins, D. A. "Predicting Dynamic Strain Amplification by Coupling a Finite Element Structural Analysis Code with a Gun Interior Ballistic Code." BRL-TR-3269, U.S. Army Ballistic Research Laboratory, Aberdeen Proving Ground, MD, September 1991.

Hallquist, J. O. "User Manual for DYNA2D - An Explicit Two-Dimensional Hydrodynamic Finite Element Code with Interactive Rezoning and Graphical Display." Lawrence Livermore National Laboratory, 1987.

Alexander, A., J. T. Tzeng, W. H. Drysdale, and B. P. Burns. "Effective Properties of 3D Laminated Composites for Finite Element Applications." Proceedings of 1994 International Conference of Computers in Engineering, vol. 2, ASME, pp. 507–518, 1994.

INTENTIONALLY LEFT BLANK.

NO. OF
COPIES   ORGANIZATION

2   DEFENSE TECHNICAL INFO CTR
         ATTN DTIC DDA
         8725 JOHN J KINGMAN RD
         STE 0944
         FT BELVOIR VA 22060-6218

1   DIRECTOR
         US ARMY RESEARCH LAB
         ATTN AMSRL OP SD TA
         2800 POWDER MILL RD
         ADELPHI MD 20783-1145

3   DIRECTOR
         US ARMY RESEARCH LAB
         ATTN AMSRL OP SD TL
         2800 POWDER MILL RD
         ADELPHI MD 20783-1145

1   DIRECTOR
         US ARMY RESEARCH LAB
         ATTN AMSRL OP SD TP
         2800 POWDER MILL RD
         ADELPHI MD 20783-1145

         ABERDEEN PROVING GROUND

5   DIR USARL
         ATTN AMSRL OP AP L (305)

1 HQDA
ATTN SARD TT DR F MILTON
PENTAGON
WASHINGTON DC 20310-0103

1 HQDA
ATTN SARD TR DR R CHAIT
PENTAGON
WASHINGTON DC 20310-0103

1 HQDA
ATTN SARD TR MS K KOMINOS
PENTAGON
WASHINGTON DC 201310-0103

1 DIRECTOR
US ARMY RESEARCH LAB
ATTN AMSRL CP CA D SNIDER
2800 POWDER MILL ROAD
ADELPHI MD 20783-1145

3 COMMANDER
US ARMY ARDEC
ATTN SMCAR TD
R PRICE
V LINDER
C SPINELLI
PCTNY ARSNL NJ 07806-5000

1 COMMANDER
US ARMY ARDEC
ATTN F MCLAUGHLIN
PCTNY ARSNL NJ 07806-5000

1 COMMANDER
US ARMY ARDEC
ATTN SMCAR CCH V E FENNELL
PCTNY ARSNL NJ 07806-5000

4 COMMANDER
US ARMY ARDEC
ATTN SMCAR CCH T
S MUSALLI
P CHRISTIAN
N KRASNOW
R CARR
PCTNY ARSNL NJ 07806-5000

1 COMMANDER
US ARMY ARDEC
ATTN SMCAR CCH J DELORENZO
PCTNY ARSNL NJ 07806-5000

2 COMMANDER
US ARMY ARDEC
ATTN SMCAR CC
J HEDDERICH
COL SINCLAIR
PCTNY ARSNL NJ 07806-5000

1 COMMANDER
US ARMY ARDEC
ATTN SMCAR CCH P J LUTZ
PCTNY ARSNL NJ 07806-5000

2 COMMANDER
US ARMY ARDEC
ATTN SMCAR FSA M
D DEMELLA
F DIORIO
PCTNY ARSNL NJ 07806-5000

9 DIRECTOR
BENET LABORATORIES
ATTN AMSTA AR CCB
C KITCHENS
J KEANE
J VASILAKIS
G FRIAR
V MONTVORI
J WRZOCHALSKI
R HASENBEIN
J BATTAGLIA
AMSTA AR CCB T S SOPOK
WATERVLIET NY 12189-4050

1 COMMANDER
WATERVLIET ARSENAL
ATTN SMCWV QAE Q C HOWD
BLDG 44
WATERVLIET NY 12189-4050

1 COMMANDER
WATERVLIET ARSENAL
ATTN SMCWV SPM T MCCLOSKEY
BLDG 25 3
WATERVLIET NY 12189-4050

1 COMMANDER
WATERVLIET ARSENAL
ATTN SMCWV QA QS K INSCO
WATERVLIET NY 12189-4050

NO. OF COPIES	ORGANIZATION	NO. OF COPIES	ORGANIZATION
1	COMMANDER US ARMY ARDEC ATTN AMSMC PBM K PCTNY ARSNL NJ 07806-5000	2	PM TMAS ATTN SFAE AR TMA COL BREGARD C KIMKER PCTNY ARSNL NJ 07806-5000
1	COMMANDER US ARMY BELVOIR RD&E CTR ATTN STRBE JBC FORT BELVOIR VA 22060-5606	1	PM TMAS ATTN SFAE AR TMA MD R KOWALSKI PCTNY ARSNL NJ 07806-5000
1	DIRECTOR US ARMY CRREL ATTN P DUTTA 72 LYME ROAD HANOVER NH 03755	1	PM TMAS ATTN SFAE AR TMA MS D GUZIEWICZ PCTNY ARSNL NJ 07806-5000
1	DIRECTOR US ARMY RESEARCH LABORATORY ATTN AMSRL WT L D WOODBURY 2800 POWDER MILL ROAD ADELPHI MD 20783-1145	2	PEO ARMAMENTS ATTN SFAE AR PM D ADAMS T MCWILLIAMS PCTNY ARSNL NJ 07806-5000
2	DIRECTOR US ARMY RESEARCH LABORATORY ATTN AMSRL MA P C WHITE J MCLAUGHLIN WATERTOWN MA 02172-0001	1	PEO FAS ATTN SFAE FAS PM H GOLDMAN PCTNY ARSNL NJ 07806-5000
4	COMMANDER US ARMY MISSILE COMMAND ATTN AMSMI RD W MCCORKLE AMSMI RD ST P DOYLE AMSMI RD ST CN T VANDIVER AMSMI RD ST WF M COLE REDSTONE ARSNL AL 35898-5247	4	PM CRUSADER ATTN LTC D ELLIS G DELCOCO J SHIELDS B MACHAK PCTNY ARSNL NJ 07806-5000
2	US ARMY RESEARCH OFFICE ATTN ANDREW CROWSON J CHANDRA PO BOX 12211 RSRH TRI PK NC 27709-2211	2	NASA LANGLEY RSRCH CTR ATTN AMSRL VS W ELBER AMSRL VS S F BARTLETT JR MAIL STOP 266 HAMPTON VA 23681-0001
2	US ARMY RESEARCH OFFICE ATTN G ANDERSON R SINGLETON PO BOX 12211 RSRH TRI PK NC 27709-2211	1	COMMANDER ARPA ATTN J KELLY B WILCOX 3701 N FAIRFAX DR ARLINGTON VA 22203-1714
2	PROJECT MANAGER SADARM PCTNY ARSNL NJ 07806-5000	1	NAVAL RESEARCH LABORATORY CODE 7393 ATTN I WOLOCK WASHINGTON DC 20375-5000

NO. OF COPIES	ORGANIZATION	NO. OF COPIES	ORGANIZATION
1	OFFICE OF NAVAL RESEARCH ATTN YAPA RAJAPAKSE MECH DIV CODE 1132SM ARLINGTON VA 22217	6	NAVAL SURFACE WARFARE CTR DAHLGREN DIVISION ATTN CODE G33 R HUBBARD 3 CP G GRAFF D HANNICK J FRAYSSE DAHLGREN VA 224488
1	DAVID TAYLOR RESEARCH CTR SHIP STRUCTURES AND PROT DEPT ATTN J CORRADO CODE 1702 BETHESDA MD 20084		
2	DAVID TAYLOR RESEARCH CTR ATTN R ROCKWELL W PHYILLAIER BETHESDA MD 20054-5000	1	DREXEL UNIVERSITY ATTN ALBERT S D WANG 32ND & CHESTNUT STRS PHILADELPHIA PA 19104
6	DIRECTOR LAWRENCE LIVERMORE NATL LAB ATTN R CHRISTENSEN S DETERESA W FENG F MAGNESS M FINGER A HOLT PO BOX 808 LIVERMORE CA 94550	2	NC STATE UNIVERSITY CIVL ENGRNG DEPT ATTN W RASDORF L SPAINHOUR PO BOX 7908 RALEIGH NC 27696-7908
		1	PENNSYLVANIA ST UNIV ATTN DAVID W JENSEN 223 N HAMMOND BLDG UNIVERSITY PK PA 16802
1	OAK RIDGE NATIONAL LAB ATTN R M DAVIS PO BOX 2008 OAK RIDGE TN 37831-6195	1	PENNSYLVANIA ST UNIV ATTN RENATA S ENGEL 245 HAMMOND BLDG UNIVERSITY PK PA 16802
1	BATTELLE PNL ATTN M SMITH PO BOX 999 RICHLAND WA 99352	1	PURDUE UNIVERSITY SCHOOL OF AERO & ASTRO ATTN C T SUN W LAFAYETTE IN 47907-1282
5	DIRECTOR SANDIA NATL LABS ATTN G BENEDETTI W KAWAHARA K PERANO D DAWSON P NIELAN APLD MECH DEPT DIV 8241 PO BOX 969 LIVERMORE CA 94550-0096	1	STANFORD UNIVERSITY DEPT OF ARNTCS & ARBLSTCS ATTN S TSAI STANFORD CA 94305
		1	UNIV OF IL AT URBANA-CHAMPAIGN NATL CTR FOR COMPOSITE MTRLS RSRCH ATTN J ECONOMY 104 S WRIGHT ST URBANA IL 61801
		1	UNIV OF KENTUCKY ATTN LYNN PENN 763 ANDERSON HALL LEXINGTON KY 40506-0046

NO. OF COPIES	ORGANIZATION	NO. OF COPIES	ORGANIZATION
1	AAI CORPORATION ATTN TECH LIBRARY PO BOX 126 HUNT VALLEY MD 21030-0126	1	INTERFEROMETRICS INC ATTN R LARRIVA VP 8150 LESSBURG PIKE VIENNA VA 22100
3	ALLIANT TECHSYSTEMS INC ATTN J BODE C CANDLAND K WARD 5901 LINCOLN DR MINNEAPOLIS MN 55346-1674	1	KAMAN SCIENCES CORP ATTN T HAYDEN PO BOX 7463 COLORADO SPRINGS CO 80933
1	ALLIANT TECHSYSTEMS INC ATTN TIM HOLMQUIST 600 SECOND STREET NE HOPKINS MN 55343	2	LORAL VOUGHT SYSTEMS ATTN G JACKSON K COOK 1701 W MARSHALL DR GRAND PRAIRIE TX 75051
1	CHAMBERLAIN MFG CORP R&D DIV ATTN M TOWNSEND 550 ESTHER STREET WATERLOO IA 50704	2	MARTIN MARIETTA CORP ATTN P DEWAR L SPONAR 230 EAST GODDARD BLVD KING OF PRUSSIA PA 19406
1	CUSTOM ANALYTICAL ENGRNG SYSTEMS INC ATTN A ALEXANDER STAR ROUTE BOX 4A FLINTSTONE MD 21530	2	OLIN CORP FLINCHBAUGH DIV ATTN E STEINER B STEWART PO BOX 127 RED LION PA 17356
3	HERCULES INCORPORATED ATTN G KUEBELER J VERMEYCHUK B MANDERVILLE JR HERCULES PLAZA WILMINGTON DE 19894	1	OLIN CORP ATTN L WHITMORE 10101 9TH ST NORTH ST PETERSBURG FL 33702
1	IAP RESEARCH INC ATTN A CHALLITA 2763 CULVER AVENUE DAYTON OHIO 45429	1	DEFENSE NUCLEAR AGENCY ATTN DR R ROHR INNOVATIVE CONCEPTS DIVISION 6801 TELEGRAPH ROAD ALEXANDRIA VA 22310-3398
6	INST FOR ADVNCD TECHNOLOGY ATTN T KIEHNE H FAIR P SULLIVAN I MCNAB S BLESS R SUBRAMANIAN 4030 2 W BRAKER LANE AUSTIN TX 78759	1	EXPEDITIONARY WARFARE DIV N85 ATTN DR FRANK SHOUP 2000 NAVY PENTAGON WASHINGTON DC 20350-2000
		1	OFFICE OF NAVAL RESEARCH ATTN MR DAVID SIEGEL 351 800 N QUINCY ST ARLINGTON VA 22217-5600

NO. OF COPIES	ORGANIZATION
1	NAVAL ORDNANCE STATION ATTN D HOLMES CODE 2011 ADVANCED SYSTEMS TECHNOLOGY BR LOUISVILLE KY 40214-5245
1	NAVAL SURFACE WARFARE CENTER ATTN JOSEPH H FRANCIS CODE G30 DAHLGREN VA 22448
1	NAVAL SURFACE WARFARE CENTER ATTN E WILKERSON CODE G32 DAHLGREN VA 22448
1	DEPT OF AEROSPACE ENGNRNG ATTN DR ANTHONY J VIZZINI UNIVERSITY OF MARYLAND COLLEGE PARK MD 20742
1	DEFENSE NUCLEAR AGENCY ATTN LTC JYUJI D HEWITT INNOVATIVE CONCEPTS DIVISION 6801 TELEGRAPH RD ALEXANDRIA VA 22310-3398
1	NOESIS INC ATTN ALLEN BOUTZ 1500 WILSON BLVD STE 1224 ARLINGTON VA 22209
1	COMMANDER ATTN DAVID LIESE NAVAL SEA SYSTEMS COMMAND 2531 JEFFERSON DAVIS HWY ARLINGTON VA 22242-5160
1	NAVAL SURFACE WARFARE CTR ATTN MARY E LACY CODE D4 17320 DAHLGREN RD DAHLGREN VA 22448-5000
1	DIRECTOR NATL INST OF STD & TECH POLYMER DIV POLYMERS RM A209 ATTN GREGORY MCKENNA GAITHERSBURG MD 20899

NO. OF COPIES	ORGANIZATION
1	US DEPT OF TRANSPORTATION ATTN GOPALA VINJAMURI OFC OF HAZARDOUS MATERIALS TCHNGLY 400 SEVENTH ST SW WASHINGTON DC 20590-0001
1	ARGONNE NATIONAL LAB ATTN JOHN M KRAMER 9700 SOUTH CASS AVE ER 207 ARGONNA IL 60439-4841

<u>ABERDEEN PROVING GROUND</u>

| 27 | DIR USARL
ATTN AMSRL MA P
    L JOHNSON 131
    T CHOU 313N
AMSRL MA PA
    D GRANVILLE (CR)
    M ROYLANCE (CR)
AMSRL MA MA G HAGNAUER (CR)
AMSRL WT P A HORST 390A
AMSRL WT PB
    E SCHMIDT 120
    P PLOSTINS 120
AMSRL WT PD
    B BURNS 390
    W DRYSDALE 390
    T BOGETTI 390
    J BENDER 390
    R KIRKENDALL 390
    D HOPKINS 390
    C HOPPEL 390
    S WILKERSON 390
    R KASTE 390
    J TZENG 390
AMSRL WT PD (ALC)
    A FRYDMAN
AMSRL WT T W MORRISON 309
AMSRL WT TA
    W GILLICH 390
    W BRUCHEY 390
AMSRL WT TC
    R COATES 309
    W DE ROSSET 309
AMSRL WT W C MURPHY 120
AMSRL WT WA B MOORE 394
AMSRL WT WC T HAUG 120 |

INTENTIONALLY LEFT BLANK.

USER EVALUATION SHEET/CHANGE OF ADDRESS

This Laboratory undertakes a continuing effort to improve the quality of the reports it publishes. Your comments/answers to the items/questions below will aid us in our efforts.

1. ARL Report Number __ARL-TR-889_____ Date of Report __October 1995_____

2. Date Report Received _____

3. Does this report satisfy a need? (Comment on purpose, related project, or other area of interest for which the report will be used.) _____

_____

_____

4. Specifically, how is the report being used? (Information source, design data, procedure, source of ideas, etc.) ____

_____

_____

5. Has the information in this report led to any quantitative savings as far as man-hours or dollars saved, operating costs avoided, or efficiencies achieved, etc? If so, please elaborate. _____

_____

_____

6. General Comments. What do you think should be changed to improve future reports? (Indicate changes to organization, technical content, format, etc.) _____

_____

_____

_____

CURRENT
ADDRESS

Organization

Name

Street or P.O. Box No.

City, State, Zip Code

7. If indicating a Change of Address or Address Correction, please provide the Current or Correct address above and the Old or Incorrect address below.

OLD
ADDRESS

Organization

Name

Street or P.O. Box No.

City, State, Zip Code

(Remove this sheet, fold as indicated, tape closed, and mail.)
(DO NOT STAPLE)